
EXPLICIT QUANTUM CIRCUITS FOR BLOCK ENCODINGS OF CERTAIN SPARSE MATRICES

A PREPRINT

Daan Camps

Applied Mathematics and Computational Research Division
 Lawrence Berkeley National Laboratory
 Berkeley, CA 94720
 dcamps@lbl.gov

Lin Lin

Department of Mathematics and Challenge Institute of Quantum Computation
 University of California at Berkeley
 Applied Mathematics and Computational Research Division
 Lawrence Berkeley National Laboratory
 Berkeley, CA 94720
 linlin@math.berkeley.edu

Roel Van Beeumen

Applied Mathematics and Computational Research Division
 Lawrence Berkeley National Laboratory
 Berkeley, CA 94720
 rvanbeeumen@lbl.gov

Chao Yang

Applied Mathematics and Computational Research Division
 Lawrence Berkeley National Laboratory
 Berkeley, CA 94720
 CYang@lbl.gov

February 6, 2023

ABSTRACT

Many standard linear algebra problems can be solved on a quantum computer by using recently developed quantum linear algebra algorithms that make use of block encodings and quantum eigenvalue / singular value transformations. A block encoding embeds a properly scaled matrix of interest A in a larger unitary transformation U that can be decomposed into a product of simpler unitaries and implemented efficiently on a quantum computer. Although quantum algorithms can potentially achieve exponential speedup in solving linear algebra problems compared to the best classical algorithm, such gain in efficiency ultimately hinges on our ability to construct an efficient quantum circuit for the block encoding of A , which is difficult in general, and not trivial even for well structured sparse matrices. In this paper, we give a few examples on how efficient quantum circuits can be explicitly constructed for some well structured sparse matrices, and discuss a few strategies used in these constructions. We also provide implementations of these quantum circuits in MATLAB.

Keywords quantum linear algebra, block encoding, quantum circuit, quantum eigenvalue transformation, quantum singular value transformation, random walk, quantum walk

1 Introduction

In recent years, a new class of quantum algorithms have been developed to solve standard linear algebra problems on quantum computers. These algorithms use the technique of block encoding Low and Chuang [2017, 2019], Gilyén et al. [2019] to embed a properly scaled matrix A of interest in a larger unitary matrix U_A so that the multiplication of A with a vector x can be implemented by applying the unitary matrix U_A to a carefully prepared initial state and performing measurements on a subset of qubits. Furthermore, if A is Hermitian, by using the technique of the quantum eigenvalue transformation, one can block encode a certain matrix polynomial $p(A)$ by another unitary $U_{p(A)}$ efficiently using U_A as the building block Low and Chuang [2017]. This procedure can be generalized to non-Hermitian matrices A using a technique called the quantum singular value transformation Gilyén et al. [2019]. The larger unitary $U_{p(A)}$ can be decomposed into a product of simpler unitaries consisting of 2×2 single qubit unitaries, multi-qubit controlled-NOTs, U_A and its Hermitian conjugate. Because approximate solutions to many large-scale linear algebra problems such as linear systems of equations, least squares problems and eigenvalue problems (produced by iterative methods) can often be expressed as $p(A)v_0$ for some initial vector v_0 , the possibility to block encode $p(A)$ will enable us to solve these problems on a quantum computer that performs unitary transformations only Gilyén et al. [2019], Lin and Tong [2020a,b], Martyn et al. [2021]. In this paper, we use the term “quantum linear algebra algorithms” to refer to such block encoding based algorithms for solving linear algebra problems on a quantum computer.

In order to implement these quantum linear algebra algorithms, we need to further express the block encoding matrix U_A as a product of simpler unitaries, i.e., we need to express U_A as an efficient quantum circuit. Although it is suggested in Berry et al. [2015], Childs et al. [2017], Low and Chuang [2017], Gilyén et al. [2019] that such a quantum circuit can be constructed in theory for certain sparse matrices, the proposed construction relies on the availability of “oracles” that can efficiently encode both the nonzero structure of A and numerical values of the nonzero matrix elements. However, for a general sparse matrix A , finding these “oracles” is entirely non-trivial. Even for sparse matrices that have a well defined non-zero structure and a small set of nonzero matrix elements, encoding the structure and matrix elements by an efficient quantum circuit is not an easy task.

In this paper, we provide a few accessible examples on how to explicitly construct efficient quantum circuits for some well structured sparse matrices. In particular, we will present some general strategies for writing down the oracles for the non-zero structure and non-zero matrix elements of these matrices. In addition to explaining the general strategies and providing circuit diagrams, we also show how these circuits can be easily constructed using a MATLAB Toolbox called QCLAB Camps and Van Beeumen [2021]. To the best of our knowledge, our work is the first to demonstrate how explicit quantum circuits can be constructed in practice to block encode structured sparse matrices. All QCLAB circuit implementation can be downloaded from <https://github.com/QuantumComputingLab/explicit-block-encodings>. The block encoding of A is not unique. We will show a few different encoding schemes and the corresponding quantum circuits. For a sparse matrix A that has at most s nonzero elements per column, which we refer to as an s -sparse matrix, the general strategies we use to construct a quantum circuit actually block encodes A/s . For many applications, the extra scaling factor $1/s$ does not introduce significant issues. However, for some applications such as a quantum walk on a graph Szegedy [2004], Childs [2010], the presence of the $1/s$ factor makes the quantum algorithm less efficient, as we will show later in this paper. For these applications, we need to use a different strategy to block encode A directly. We will show how this can be done for a quantum walk in which the matrix A is a symmetric stochastic matrix or a discriminant matrix, and the corresponding quantum walk can be viewed as a block encoding of a Chebyshev polynomial of the discriminant matrix associated with the stochastic matrix A used to describe the corresponding random walk.

This paper is organized as follows. In section 3, we give a formal definition of a block encoding of a matrix A and the possibility of using the quantum eigenvalue transformation to block encode $p(A)$ for some polynomial $p(t)$. In section 4, we discuss how to construct a block encoding circuit for a scaled s -sparse matrix A/s , and give two specific examples. We discuss the possibility to use the techniques presented in section 4 to construct a circuit for the block encoding of P/s in section 5, where P is a symmetric stochastic matrix associated with a random walk. We show this circuit can be used as a building block to construct a circuit for performing a quantum walk associated with such a random walk. We explain why such a construction leads to a loss of quantum efficiency due to the $1/s$ scaling factor produced in the block encoding schemes used in section 4. An alternative approach that takes advantage of the stochastic property of a random walk and block encodes P directly instead of P/s is presented. As a result, we can construct an efficient block encoding for a Chebyshev polynomial of P . The block encoding view of a quantum walk introduced in this section differs from how quantum walks (in particular the Szegedy quantum walks Szegedy [2004]) are traditionally introduced. We make a clear connection between these two views in section 5 and show in the supplementary materials how the block encoding view can be used to explain the efficiency of a quantum walk compared a classical random walk.

2 Notations and Conventions

Following standard conventions used in the quantum computing literature, we use the Dirac $\langle \cdot |$ and $| \cdot \rangle$ notation to denote respectively row and column vectors. In particular $|0\rangle$ and $|1\rangle$ are used to represent the unit vectors $e_0 = [1 \ 0]^T$ and $e_1 = [0 \ 1]^T$, respectively. The tensor product of m $|0\rangle$'s is denoted by $|0^m\rangle$. We use $|x, y\rangle$ to represent the Kronecker product of $|x\rangle$ and $|y\rangle$, which is also sometimes written as $|x\rangle |y\rangle$ or $|xy\rangle$. The $N \times N$ identity matrix is denoted by I_N and we sometimes drop the subscript N when the dimension is clear from the context. The j th column of I_N is denoted by $|j\rangle$ for $j = 0, 1, 2, \dots, N - 1$. For the binary representation of $j \in \mathbb{N} : 0 \leq j \leq 2^n - 1$, we use the *little-endian* convention as given by

$$j = [j_{n-1} \cdots j_1 j_0] = j_{n-1} \cdot 2^{n-1} + \cdots + j_1 \cdot 2^1 + j_0 \cdot 2^0,$$

where $j_i \in \{0, 1\}$ for $i = 0, \dots, n - 1$.

We use the letters H , X , Y , and Z to represent the Hadamard, Pauli- X , Pauli- Y , and Pauli- Z matrices, respectively, defined below

$$H = \frac{1}{\sqrt{2}} \begin{bmatrix} 1 & 1 \\ 1 & -1 \end{bmatrix}, \quad X = \begin{bmatrix} 0 & 1 \\ 1 & 0 \end{bmatrix}, \quad Y = \begin{bmatrix} 0 & -i \\ i & 0 \end{bmatrix}, \quad Z = \begin{bmatrix} 1 & 0 \\ 0 & -1 \end{bmatrix}. \quad (2.1)$$

Further, rotation matrices along the Pauli- Y axis will play a key role in the construction of block encoding circuits and are defined as follows

$$R_y(\theta) := \begin{bmatrix} \cos\left(\frac{\theta}{2}\right) & -\sin\left(\frac{\theta}{2}\right) \\ \sin\left(\frac{\theta}{2}\right) & \cos\left(\frac{\theta}{2}\right) \end{bmatrix} = e^{-i\theta Y/2}, \quad (2.2)$$

where θ is the rotation angle and the unitary Y defined in (2.1). The matrices in eqs. (2.1) and (2.2) are 2×2 unitaries and serve as basic single qubit quantum gates.

We follow the standard convention for drawing quantum circuits with multiple parallel lines covered by several layers of rectangular boxes. Each line corresponds to either a single qubit or multiple qubits depending on how it is labelled and each box corresponds to a single qubit or multi-qubit gate depending on the number of qubit lines passing through it. We use the convention that the qubits in a circuit diagram are numbered increasingly from the top to the bottom as illustrated by the 3 qubit circuit U in fig. 1a. An integer $j = [j_{n-1} \cdots j_1 j_0]$ input to a circuit is prepared as a set of quantum states $|j_{n-1}\rangle, \dots, |j_0\rangle$ with $|j_0\rangle$ mapped to the highest numbered qubit q_{n-1} and $|j_{n-1}\rangle$ mapped to the lowest numbered qubit q_0 , see e.g., fig. 1b.

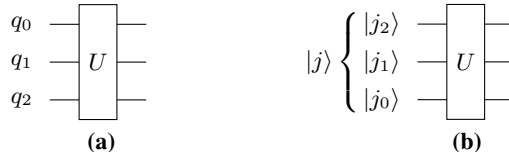


Figure 1. (a) Qubits of a quantum circuit U are numbered increasingly from the top to the bottom. (b) How the binary representation of an integer (j) input is mapped to the qubits of the quantum circuit U .

An important class of quantum gates are the controlled gates, i.e., one or more qubits act as a control for some operation. Graphically, the control operation is represented by a vertical line connecting the control qubit(s), marked by either a solid or open circle, to the so called target gate, see e.g., the controlled NOT (CNOT) in fig. 2. The target can also be multiple gates grouped in a subcircuit block used to perform certain operations. A solid circle indicates that the controlled operation is performed on the connected qubit, when the input to the controlling qubit is a $|1\rangle$ state. Similarly, an open circle indicates that the controlled operation is performed when the input to the controlling qubit is a $|0\rangle$ state.

Figure 2. Controlled-NOT gates.

Mathematically, the controlled gates from fig. 2 translate into

$$E_0 \otimes X + (I - E_0) \otimes I, \quad \text{and} \quad E_1 \otimes X + (I - E_1) \otimes I, \quad (2.3)$$

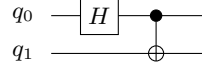
respectively, where the orthogonal projection operators

$$E_0 = e_0 e_0^T = |0\rangle\langle 0|, \quad E_1 = e_1 e_1^T = |1\rangle\langle 1|, \quad (2.4)$$

serve as the controls. Note that the NOT (X) operation is applied to the input of qubit q_1 in fig. 2a only if the input to qubit q_0 is $|0\rangle$. Likewise, the NOT operation is applied to the input of qubit q_1 in fig. 2b if the input to qubit q_0 is $|1\rangle$. A similar expression can be used to denote multi-qubit controlled NOT gates.

Throughout this paper, we use the QCLAB Toolbox¹ to construct and draw quantum circuits for block encodings of matrices in MATLAB. Hence, it will be convenient to verify that a presented quantum circuit performs the correct unitary transformation. As a simple example, the following listing constructs a simple quantum circuit with $n = 2$ qubits that prepares a so-called Bell state when the input of the circuit is $|00\rangle$. The circuit consists of a Hadamard gate on the first qubit, followed by a CNOT gate with control on the first and target on the second qubit.

```
circuit = qclab.QCircuit(2);
circuit.push_back(qclab.qgates.Hadamard(0));
circuit.push_back(qclab.qgates.CNOT(0,1));
```



QCLAB uses MATLAB's object oriented programming capabilities to keep track of all gates used in the circuit and to which qubits these gates are applied to and in what order. The first line of the listing defines a QCLAB circuit object `circuit` consisting of 2 qubits. The circuit is constructed by using the `push_back` function to place quantum gates (`qgates`) one layer at a time into the `circuit` object according to the circuit diagram shown to the right of the listing. The unitary matrix defined by the circuit is not explicitly formed unless the `circuit.matrix` function is called. One can also draw a circuit by using the `circuit.draw` function. We refer readers to the User's manual of QCLAB Camps and Van Beeumen [2021] for the syntax of its usage.

3 Block encoding and quantum eigenvalue transformation

Block encoding is a technique for embedding a properly scaled nonunitary matrix $A \in \mathbb{C}^{N \times N}$ into a unitary matrix U_A of the form

$$U_A = \begin{bmatrix} A & * \\ * & * \end{bmatrix}, \quad (3.1)$$

where $*$ denotes a matrix block yet to be determined. Applying U_A to a vector of the form

$$v = \begin{bmatrix} x \\ 0 \end{bmatrix} = |0\rangle|x\rangle, \quad (3.2)$$

where $\|x\|_2 = 1$, yields

$$w = U_A v = \begin{bmatrix} Ax \\ * \end{bmatrix} = |0\rangle(A|x\rangle) + |1\rangle|*\rangle,$$

where $*$ here denotes a vector that we do not care about. If we measure the first qubit and obtain the $|0\rangle$ state, the second qubit register then contains $A|x\rangle$. The probability of such a successful measurement is $\|Ax\|^2$.

Note that by "a properly scaled A ", we mean that A is scaled to satisfy $\|A\|_2 \leq 1$. Without such a scaling, a block encoding of A may not exist because the singular values of any submatrix blocks of a unitary matrix must be bounded by 1. Furthermore, if there are some constraints on the type of unitary we can construct, e.g., the type of quantum gates available on a quantum computer, we may not be able to find a U_A that block encodes A exactly. However, in this paper, we assume that A has already been properly scaled, and there is no constraints on the quantum gates we can use to construct a quantum circuit representation of the unitary matrix U_A .

To give an example of a block encoding, let us consider a 1×1 matrix $A = \alpha$, where $0 < \alpha < 1$. In this extremely simple case, a block encoding of A can be constructed as

$$U_A = \begin{bmatrix} \alpha & \sqrt{1-\alpha^2} \\ \sqrt{1-\alpha^2} & -\alpha \end{bmatrix}, \quad \text{or} \quad U_A = \begin{bmatrix} \alpha & -\sqrt{1-\alpha^2} \\ \sqrt{1-\alpha^2} & \alpha \end{bmatrix}. \quad (3.3)$$

¹QCLAB Toolbox: <https://github.com/QuantumComputingLab/qclab>

Although this type of block encoding can be extended to a properly scaled matrix A of a larger dimension to yield

$$U_A = \begin{bmatrix} A & (I - A^\dagger A)^{1/2} \\ (I - A^\dagger A)^{1/2} & -A \end{bmatrix}, \text{ or } \begin{bmatrix} A & -(I - A^\dagger A)^{1/2} \\ (I - A^\dagger A)^{1/2} & A \end{bmatrix}, \quad (3.4)$$

this approach is not practical because it requires computing the square root of $A^\dagger A$, which requires computing and diagonalizing $A^\dagger A$. In general, there is no efficient algorithm to perform these operations on a quantum computer using $\mathcal{O}(\text{poly}(n))$ quantum gates.

A more practical scheme that does not require computing the square root of A can be illustrated by the following real symmetric 2×2 example. Let

$$A = \begin{bmatrix} \alpha_1 & \alpha_2 \\ \alpha_2 & \alpha_1 \end{bmatrix}, \quad (3.5)$$

where $|\alpha_1|, |\alpha_2| \leq 1$. It can be verified that the matrix

$$U_A = \frac{1}{2} \begin{bmatrix} U_\alpha & -U_\beta \\ U_\beta & U_\alpha \end{bmatrix} \quad (3.6)$$

is a block encoding of $A/2$, where

$$U_\alpha = \begin{bmatrix} \alpha_1 & \alpha_2 & \alpha_1 & -\alpha_2 \\ \alpha_2 & \alpha_1 & -\alpha_2 & \alpha_1 \\ \alpha_1 & -\alpha_2 & \alpha_1 & \alpha_2 \\ -\alpha_2 & \alpha_1 & \alpha_2 & \alpha_1 \end{bmatrix}, \quad U_\beta = \begin{bmatrix} \beta_1 & \beta_2 & \beta_1 & -\beta_2 \\ \beta_2 & \beta_1 & -\beta_2 & \beta_1 \\ \beta_1 & -\beta_2 & \beta_1 & \beta_2 \\ -\beta_2 & \beta_1 & \beta_2 & \beta_1 \end{bmatrix}, \quad (3.7)$$

with $\beta_1 = \sqrt{1 - \alpha_1^2}$ and $\beta_2 = \sqrt{1 - \alpha_2^2}$. To implement this unitary on a quantum computer, we must further decompose U_A as a product of simpler unitaries and construct a quantum circuit with a limited number of quantum gates. We will discuss how to construct such a quantum circuit in the next section. The method for constructing the block encoding shown in (3.6)–(3.7) cannot be easily generalized to matrices of larger dimensions. However, for matrices with special structures, e.g., sparse matrices, it is possible to develop some general block encoding strategies which we will discuss in the next section. The general definition of a block encoding is as follows.

Definition 3.1 (Block encoding). *Given an n -qubit matrix A ($N = 2^n$), if we can find $\alpha, \epsilon \in \mathbb{R}_+$, and an $(m+n)$ -qubit unitary matrix U_A so that*

$$\|A - \alpha (\langle 0^m | \otimes I_N) U_A (|0^m \rangle \otimes I_N)\|_2 \leq \epsilon, \quad (3.8)$$

then U_A is called an (α, m, ϵ) -block-encoding of A . In particular, when the block encoding is exact with $\epsilon = 0$, U_A is called an (α, m) -block-encoding of A .

Here m is the number of ancilla qubits used to block encode A , and the expression $(\langle 0^m | \otimes I_N) U_A (|0^m \rangle \otimes I_N)$ should be interpreted as taking the upper-left $2^n \times 2^n$ matrix block of U_A . For example, the block encoding in (3.6)–(3.7) is a $(1, 2)$ -block-encoding of A in eq. (3.5).

When solving a large and sparse linear algebra problem on a classical computer, we often use an iterative solver to seek an approximate solution \hat{x} . For simplicity we assume A is Hermitian. In many cases, such as when a Krylov subspace method is used, the approximate solution can be written as $\hat{x} = p(A)v_0$, where $p(t)$ is a polynomial that approximates a desired function and v_0 is an initial guess or simply a random vector. For example, to solve a linear system of equations $Ax = b$, we choose $p(t)$ to be a polynomial approximation to $1/t$ on the spectrum of A and $v_0 = b$.

To solve this problem on a quantum computer using the technique of block encoding, we need to block encode the matrix function $p(A)$. If we are provided a $(1, m)$ -block-encoding of the Hermitian matrix A denoted by U_A , this task can be achieved by a quantum eigenvalue transformation (QET) Low and Chuang [2017], Gilyén et al. [2019]. Specifically, for any real polynomial $p(t)$ of degree d satisfying (i) the parity of p is $(d \bmod 2)$, and (ii) $|p(t)| \leq 1, \forall t \in [-1, 1]$, there exists a set of parameters $\{\phi_i\}_{i=0}^d \in \mathbb{R}^{d+1}$ so that the quantum circuit in fig. 3 provides a $(1, m+1)$ -block-encoding of $p(A)$ [Gilyén et al., 2019, Corollary 11] denoted by $U_{p(A)}$.

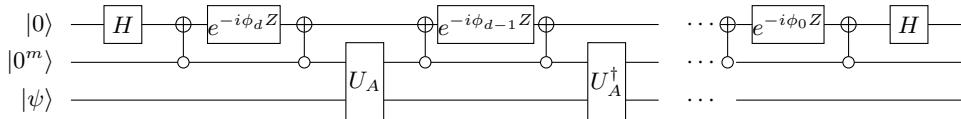


Figure 3. A quantum circuit for the block encoding of $p(A)$.

The QET theory and the corresponding quantum circuit for block encoding a polynomial of A in terms of the block encoding of A is a consequence of quantum signal processing (QSP) Low and Chuang [2017], Gilyén et al. [2019], which represents a scalar polynomial of degree d using a product of unitary matrices of size 2×2 , parameterized by $(d + 1)$ real numbers called the phase factors. We state the result of QSP below for completeness, which is a slight variation of [Gilyén et al., 2019, Theorem 4].

Theorem 3.2 (Quantum signal processing). *Let*

$$U(t) = \begin{bmatrix} t & \sqrt{1-t^2} \\ \sqrt{1-t^2} & -t \end{bmatrix}. \quad (3.9)$$

There exists a set of phase angles $\Phi_d \equiv \{\phi_0, \dots, \phi_d\} \in \mathbb{R}^{d+1}$ so that

$$U_{\Phi_d}(t) \equiv e^{i\phi_0 Z} \prod_{j=1}^d [U(t)e^{i\phi_j Z}] = \begin{bmatrix} p(t) & -q(t)\sqrt{1-t^2} \\ q^*(t)\sqrt{1-t^2} & p^*(t) \end{bmatrix}, \quad (3.10)$$

if and only if $p(t)$ and $q(t)$ are complex valued polynomials in t and satisfy

1. $\deg(p) \leq d$, $\deg(q) \leq d - 1$;
2. p has parity d mod 2 and q has parity $d - 1$ mod 2;
3. $|p(t)|^2 + (1 - t^2)|q(t)|^2 = 1$, $\forall t \in [-1, 1]$.

When $d = 0$, $\deg(q) \leq -1$ should be interpreted as $q = 0$.

We may verify that if $\Phi_d \equiv (\phi_0, \phi_1, \dots, \phi_d)$ is chosen as

$$\phi_j = \begin{cases} \pi/4, & j = 0 \text{ or } d \\ \pi/2, & j = 1, \dots, d - 1 \end{cases}$$

then $p(t)$ is the d th degree Chebyshev polynomial of the first kind (up to a constant global factor i^d). However, for a properly normalized arbitrary d th degree (real valued) polynomial $p(t)$, finding the phase angles in $\Phi_d \equiv (\phi_0, \phi_1, \dots, \phi_d)$ to make (3.10) hold is not trivial. In the past few years, there has been significant progress in developing new algorithms to improve the efficiency and robustness to find phase factors Gilyén et al. [2019], Haah [2019], Chao et al. [2020], Dong et al. [2021], Ying [2022], Dong et al. [2022].

The approach adopted in this paper is the optimization based method Dong et al. [2021], which computes the phase angles $\phi_0, \phi_1, \dots, \phi_d$ by solving the nonlinear least squares problem

$$\min_{\Phi_d} \sum_{k=1}^{\tilde{d}} |\Re[e_1^T U_{\Phi_d}(t_k) e_1] - p_d(t_k)|^2,$$

where t_k are chosen to be roots of a Chebyshev polynomial, and $\tilde{d} = \lceil (d + 1)/2 \rceil$. This approach is particularly useful when we are targeting a *real* polynomial $p(t)$. With a proper choice of the initial guess, and despite the complex global optimization landscape Wang et al. [2022], this approach can robustly find phase factors for high degree polynomials ($d \sim 10^4$).

Once we have an efficient quantum circuit to construct the block encoding U_A , we can easily construct an efficient quantum circuit for $U_{p(A)}$. For a general matrix A , the quantum circuit in fig. 3 no longer corresponds to a QET, but a quantum singular value transformation (QSVT) of A (see Gilyén et al. [2019] for more detailed discussion of QSVT).

In the next section, we will focus on techniques for constructing an efficient quantum circuit for U_A associated with a well structured sparse A .

4 Efficient quantum circuits for block encodings of s -sparse matrices

In this section, we introduce strategies to directly construct quantum circuits for block encodings of structured and sparse matrices. Before diving into all the details, we first return to real symmetric 2×2 example of (3.5). If we define $\phi_1 = \arccos(\alpha_1) + \arccos(\alpha_2)$ and $\phi_2 = \arccos(\alpha_1) - \arccos(\alpha_2)$, then we can verify that the block encoding (3.6)–(3.7) for the 2×2 matrix (3.5) can be factored as a product of simpler unitaries, i.e.,

$$U_A = U_6 U_5 U_4 U_3 U_2 U_1 U_0, \quad (4.1)$$

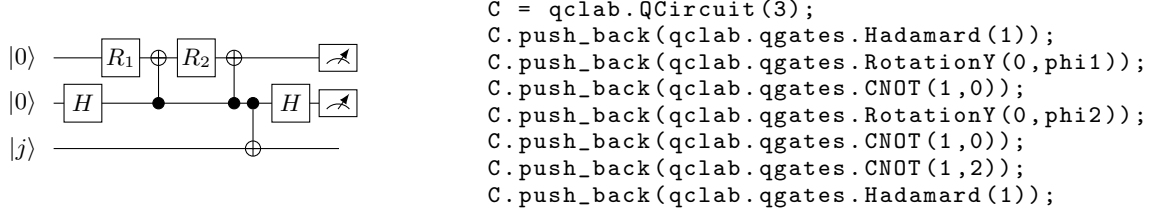


Figure 4. A quantum circuit for the block encoding of a 2×2 symmetric matrix A .

where $U_0 = U_6 = I_2 \otimes H \otimes I_2$, $U_1 = R_1 \otimes I_2 \otimes I_2$, $U_2 = U_4 = (I_2 \otimes E_0 + X \otimes E_1) \otimes I_2$, $U_3 = R_2 \otimes I_2 \otimes I_2$, and $U_5 = I_2 \otimes (E_0 \otimes I_2 + E_1 \otimes X)$. Here, H , X are the Hadamard and Pauli- X gates defined in (2.1), $R_1 = R_y(\phi_1)$, $R_2 = R_y(\phi_2)$ are the rotation matrices defined in (2.2), and E_0 , E_1 are projectors defined in (2.4). The quantum circuit associated with the factorization given in (4.1) is shown in fig. 4.

Note that in this case, the quantum circuit requires 2 ancilla qubits in addition to the $n = 1$ system qubit required to match the dimension of A , which is $N = 2^n$. As a result, the unitary that block encodes the 2×2 matrix A is of dimension 2^3 , which is twice the dimension of the block encoding given by (3.4).

Although it may not be immediately clear how (4.1) and the corresponding quantum circuit shown in fig. 4 are obtained from the block encoding matrix (3.6)–(3.7), it is possible, as we will show below, to develop a general scheme to construct a block encoding and the corresponding quantum circuit for well-structured matrices. In particular, when the matrix A is sparse with a structured sparsity pattern and the nonzero matrix elements can also be well characterized, an efficient block encoding circuit for A can be constructed, as we will show in the next section.

In the following, we will focus on an s -sparse matrix, which is defined to be a sparse matrix with at most s nonzeros in each column and row. For simplicity, let us assume $s = 2^m \ll N$ for some integer $m \ll n$. When s is not a power of 2, we can always increase s to a power of 2 by treating some zeros as nonzeros. The following theorem, which is a variant of [Gilyén et al., 2019, Lemma 48 (in the full version)], asserts that such a sparse matrix can be block encoded if we can construct unitaries that can encode both the nonzero structure and the nonzero matrix elements of A .

Theorem 4.1. *Let $c(j, \ell)$ be a function that gives the index of the ℓ th non-zero element in the j th column of an s -sparse matrix $A \in \mathbb{C}^{N \times N}$ with $N = 2^n$, where $s = 2^m$. If there exists a unitary O_c such that*

$$O_c |\ell\rangle |j\rangle = |\ell\rangle |c(j, \ell)\rangle, \quad (4.2)$$

and a unitary O_A such that

$$O_A |0\rangle |\ell\rangle |j\rangle = \left(A_{c(j, \ell), j} |0\rangle + \sqrt{1 - |A_{c(j, \ell), j}|^2} |1\rangle \right) |\ell\rangle |j\rangle, \quad (4.3)$$

then

$$U_A = (I_2 \otimes D_s \otimes I_N) (I_2 \otimes O_c) O_A (I_2 \otimes D_s \otimes I_N), \quad (4.4)$$

block encodes A/s . Here D_s is called a diffusion operator and is defined as

$$D_s \equiv \underbrace{H \otimes H \otimes \cdots \otimes H}_m, \quad (4.5)$$

Proof. Note that applying D_s to $|0^m\rangle$ yields

$$D_s |0^m\rangle = \frac{1}{\sqrt{s}} \sum_{\ell=0}^{s-1} |\ell\rangle,$$

where $\{|\ell\rangle\}$ forms the computational basis in the Hilbert space defined by m qubits. Our goal is to show that $\langle 0 | \langle 0^m | \langle i | U_A | 0 \rangle | 0^m \rangle | j \rangle = A_{ij}/s$. In order to compute the inner product $\langle 0 | \langle 0^m | \langle i | U_A | 0 \rangle | 0^m \rangle | j \rangle$, we apply D_s, O_A, O_c to $|0\rangle |0^m\rangle |j\rangle$ successively as illustrated below

$$\begin{aligned}
|0\rangle |0^m\rangle |j\rangle &\xrightarrow{D_s} \frac{1}{\sqrt{s}} \sum_{\ell \in [s]} |0\rangle |\ell\rangle |j\rangle \\
&\xrightarrow{O_A} \frac{1}{\sqrt{s}} \sum_{\ell \in [s]} \left(A_{c(j, \ell), j} |0\rangle + \sqrt{1 - |A_{c(j, \ell), j}|^2} |1\rangle \right) |\ell\rangle |j\rangle \\
&\xrightarrow{O_c} \frac{1}{\sqrt{s}} \sum_{\ell \in [s]} \left(A_{c(j, \ell), j} |0\rangle + \sqrt{1 - |A_{c(j, \ell), j}|^2} |1\rangle \right) |\ell\rangle |c(j, \ell)\rangle,
\end{aligned} \quad (4.6)$$

where $[s]$ denotes the set of integers $\{0, 1, \dots, s - 1\}$. Instead of multiplying the leftmost factor $I_2 \otimes D_s \otimes I_N$ in (4.4) to last line of (4.6), we apply it to $|0\rangle|0^m\rangle|i\rangle$ first to obtain

$$|0\rangle|0^m\rangle|i\rangle \xrightarrow{D_s} \frac{1}{\sqrt{s}} \sum_{\ell' \in [s]} |0\rangle|\ell'\rangle|i\rangle. \quad (4.7)$$

Finally, taking the inner product between (4.6) and (4.7) yields

$$\langle 0| \langle 0^m | \langle i | U_A | 0 \rangle | 0^m \rangle | j \rangle = \frac{1}{s} \sum_{\ell} A_{c(j, \ell), j} \delta_{i, c(j, \ell)} = \frac{1}{s} A_{ij}. \quad (4.8)$$

□

The quantum circuit associated with the block encoding defined in theorem 4.1 is shown in fig. 5. Note that the implementation of this block encoding requires $m + 1$ ancilla qubits in addition to n system qubits. In order to turn this into an efficient quantum circuit, we need to further decompose the O_c and O_A unitaries into a sequence of quantum gates, which may not be straightforward. In the circuit shown in fig. 4 which corresponds to the decomposition given in (4.1), O_A is decomposed as $O_A = U_4 U_3 U_2 U_1$ and O_C is simply U_5 . We will show how these decompositions are constructed systematically in the next section.

Although it may be possible to construct a set of controlled quantum gates to achieve (4.2) and (4.3) for a specific pair of j and ℓ . This approach will not yield an efficient quantum circuit because the total number of quantum gates in the circuit will be on the order of $\mathcal{O}(N)$, which is exponential with respect to n . Other brute-force approaches such as the one proposed in Camps and Van Beeumen [2022] may also require $\mathcal{O}(N)$ gates. Our goal is to construct a circuit that has a gate complexity of $\text{poly}(n)$, i.e., a polynomial in n , at least for certain sparse and/or structured matrices with well defined sparsity patterns.

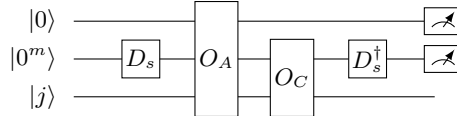


Figure 5. A general schematic circuit drawing for the block encoding of an s -sparse matrix A .

Note that O_C is unitary. According to eq. (4.2), we must have $O_C^\dagger |\ell\rangle |c(j, \ell)\rangle = |\ell\rangle |j\rangle$. This means that for each row index $i = c(j, \ell)$, we can recover the column index j given the value of ℓ . This assumption is of course somewhat restrictive, but it covers important cases such as banded matrices. For more general query models we refer readers to Gilyén et al. [2019]. We remark that it can generally be more difficult to explicitly construct quantum circuits for O_C 's in these more general query models.

In the following, we give some specific examples to illustrate how efficient quantum circuits for O_C and O_A can be constructed for some well structured sparse matrices.

4.1 Real symmetric 2×2 matrix

We revisit the matrix (3.5) once more and view it as an s -sparse matrix with $s = 2$ even though it is dense. Therefore, we can still use the recipe given in theorem 4.1 to construct a block encoding of $A/2$. We will show below how explicit circuits for O_C and O_A can be constructed.

4.1.1 The O_C circuit

Since the second column of (3.5) is a down or up shift of the first one, the function $c(j, \ell)$, which defines the (0-based) row index of the ℓ th nonzero element in the j th column, can be defined by

$$c(j, \ell) = \text{mod}(j + \ell, 2), \quad (4.9)$$

for $j, \ell = \{0, 1\}$. After enumerating of all possible combinations of (ℓ, j) input pairs and their corresponding $(\ell, c(j, \ell))$ output pairs shown in (4.10) (on the right), we see that O_C can be simply implemented as a CNOT gate shown on the

left of (4.10).

$$\begin{array}{c} |0\rangle \xrightarrow{O_C} |0\rangle \\ |1\rangle \xrightarrow{O_C} |1\rangle \end{array} = \begin{array}{c} \text{Control} \\ \text{Target} \end{array} \quad \begin{array}{c} \ell \ j \\ \hline 0 \ 0 \\ 0 \ 1 \\ 1 \ 0 \\ 1 \ 1 \end{array} \rightarrow \begin{array}{c} \ell \ c(j, \ell) \\ \hline 0 \ 0 \\ 0 \ 1 \\ 1 \ 1 \\ 1 \ 0 \end{array} \quad (4.10)$$

using the following two lines QCLAB code

```
QC = qclab.QCircuit(2,1);
QC.push_back(qclab.qgates.CNOT(0,1));
```

4.1.2 The O_A circuit

The basic strategy to construct a circuit for O_A defined by (4.3) is to use controlled rotations to place numerical values at proper locations in U_A . Because the matrix A in (3.5) has at most two unique matrix elements. We need two controlled rotations. In general, we need to condition the application of these rotations on the values of j and ℓ . However, since the values of α_1 and α_2 in (3.5) depend solely on ℓ , control is only required on the qubit that takes $|\ell\rangle$ as the input. We apply the rotation $R_y(\theta_1)$ with $\theta_1 = 2 \arccos(\alpha_1)$ when $\ell = 0$, and $R_y(\theta_2)$ with $\theta_2 = 2 \arccos(\alpha_2)$ when $\ell = 1$. These controlled rotations are combined to yield the following O_A circuit.

$$\begin{array}{c} |0\rangle \xrightarrow{O_A} |0\rangle \\ |\ell\rangle \xrightarrow{O_A} |0\rangle \\ |j\rangle \xrightarrow{O_A} |0\rangle \end{array} = \begin{array}{c} \text{Control} \\ \text{Target} \end{array} \quad \begin{array}{c} R_y(\theta_1) \quad R_y(\theta_2) \\ \hline \text{Control} \quad \text{Control} \\ \text{Control} \quad \text{Control} \end{array} \quad \begin{array}{c} \theta_1 = 2 \arccos(\alpha_1) \\ \theta_2 = 2 \arccos(\alpha_2) \end{array} \quad (4.11)$$

Note that the last qubit is not used in this O_A circuit. The corresponding QCLAB code is given by

```
OA = qclab.QCircuit(3);
OA.push_back(qclab.qgates.CRotationY(1,0,theta1,0));
OA.push_back(qclab.qgates.CRotationY(1,0,theta2,1));
```

On some quantum hardware, it is preferable to use single qubit rotation and CNOT gates in place of controlled rotation gates. These are sometimes referred to as *uniformly controlled rotations* Möttönen et al. [2004]. In (4.12), we show how the controlled rotations used in the O_A circuit (4.11) can be replaced by an equivalent set of uniformly controlled rotation gates.

$$\begin{array}{c} R_y(\theta_1) \quad R_y(\theta_2) \\ \hline \text{Control} \quad \text{Control} \end{array} = \begin{array}{c} R_y(\phi_1) \oplus R_y(\phi_2) \oplus \\ \text{Control} \quad \text{Control} \end{array} \quad \begin{array}{c} \theta_1 = \phi_1 + \phi_2 \\ \theta_2 = \phi_1 - \phi_2 \end{array} \quad (4.12)$$

The desired uniformly controlled rotations can be constructed in QCLAB by

```
OA = qclab.QCircuit(3);
OA.push_back(ucry([theta1,theta2]));
```

To see that the right hand side of (4.12) is identical to the left hand, we observe first that, if the second qubit is in the $|0\rangle$ state, the circuit on the left applies $R_y(\theta_1)$ to the first qubit. In the circuit on the right, $R_y(\phi_2)R_y(\phi_1)$ is applied to the first qubit in this case. These two operations are identical when $\theta_1 = \phi_1 + \phi_2$. Secondly, if the second qubit is in the $|1\rangle$ state, the left circuit applies $R_y(\theta_2)$ to the first qubit, while the right circuit applies the gate sequence $XR_y(\phi_2)XR_y(\phi_1)$. It follows from the identity $XR_y(\theta)X = R_y(-\theta)$ that these operations are equivalent if $\theta_2 = \phi_1 - \phi_2$.

4.1.3 The complete circuit

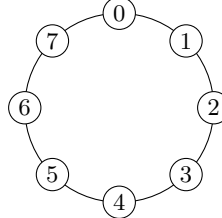
Finally, we substitute circuits eqs. (4.10) and (4.12), together with $D_s = H$ into fig. 5 and obtain the complete block-encoding quantum circuit for the matrix (3.5). Note that this circuit is identical to the one we have already introduced in fig. 4.

4.2 Banded circulant matrix

A sparse matrix A can be viewed as an adjacency matrix for a directed graph defined in terms a vertex set V , which consists of column indices $\{j\}$ of A , and an edge set E , which consists of pairs of indices $\{(i, j)\}$. The (i, j) th element

of A is nonzero if $(i, j) \in E$. The numerical value of the (i, j) th element of A , denoted by $A_{i,j}$, represents the weight of the edge emanating from the vertex j and incident to the vertex i for a directed graph. For an undirected graph, the corresponding adjacency matrix is symmetric, i.e., $A_{i,j} = A_{j,i}$.

In this subsection, we will focus on the sparse matrix associated with a directed cyclic graph. To illustrate this, we consider the following cyclic graph with $N = 8$ vertices and associated banded circulant adjacency matrix



$$A = \begin{bmatrix} \alpha & \gamma & 0 & \cdots & \beta \\ \beta & \alpha & \ddots & \ddots & 0 \\ 0 & \beta & \ddots & \gamma & \vdots \\ \vdots & \ddots & \ddots & \alpha & \gamma \\ \gamma & 0 & \cdots & \beta & \alpha \end{bmatrix}. \quad (4.13)$$

Although not shown explicitly in (4.13), two directed edges emanate from each vertex j , $0 \leq j \leq N - 1$, i.e., $(\text{mod}(j + 1, N), j) \in E$ and $(j, \text{mod}(j - 1, N)) \in E$. The weights associated with these edges are β and γ . We also assign a weight α to each vertex. This weight can also be viewed as the weight associated with a self-loop edge from a vertex j to itself. The matrix is nearly tridiagonal with the value α on its diagonal, γ on its superdiagonal and β on the subdiagonal. The non-zero elements $A_{N-1,0} = \gamma$ and $A_{0,N-1} = \beta$ reflect the cyclic feature of the graph. Each column of the matrix has 3 nonzeros. We use $m = \lceil \log_2 3 \rceil = 2$ ancilla qubits to encode the row indices of the nonzero matrix elements in each column. An additional ancilla qubit is needed to encode the numerical values of the nonzero matrix elements. When using theorem 4.1 to construct the block encoding circuit, we take $s = 2^m = 4$ here, i.e., we view (4.13) as a 4-sparse matrix even though each column of the matrix has only 3 nonzero matrix elements.

4.2.1 The O_C circuit

For the sparse adjacency matrix induced by the cyclic graph, the function $c(j, \ell)$, which defines the row index of the ℓ th nonzero element in the j th column, can be written as

$$c(j, \ell) = \text{mod}(j + \ell - 1, N) = \begin{cases} \text{mod}(j - 1, N) & \text{if } \ell = 0 \text{ (superdiagonal),} \\ j & \text{if } \ell = 1 \text{ (diagonal) or } 3, \\ \text{mod}(j + 1, N) & \text{if } \ell = 2 \text{ (subdiagonal).} \end{cases} \quad (4.14)$$

Therefore, to implement the O_C unitary defined in (4.2), we need to construct a circuit to map $|j\rangle$ to $|\text{mod}(j - 1, N)\rangle$, $|j\rangle$, or $|\text{mod}(j + 1, N)\rangle$ depending on the value of $\ell = \{0, 1, 2\}$. These cyclic subtraction and addition mappings are simply left and right shift permutation operators defined as

$$L = \begin{bmatrix} 0 & 0 & \dots & \dots & 1 \\ 1 & 0 & 0 & \ddots & 0 \\ \vdots & 1 & \ddots & \ddots & \vdots \\ \vdots & \ddots & \ddots & \ddots & \vdots \\ 0 & 0 & \dots & 1 & 0 \end{bmatrix}, \quad R = \begin{bmatrix} 0 & 1 & \dots & \dots & 0 \\ 0 & 0 & 1 & \ddots & 0 \\ \vdots & \ddots & \ddots & \ddots & \vdots \\ \vdots & \ddots & \ddots & \ddots & 1 \\ 1 & 0 & \dots & \ddots & 0 \end{bmatrix}. \quad (4.15)$$

Note that the L and R operators correspond to the addition and subtraction arithmetic operations, i.e., $+1$ and -1 , respectively. They can be implemented by a quantum circuit consisting of multi-qubit controlled-NOT gates shown in figs. 6a and 6b. The multi-qubit controlled gates perform the carry operation in the binary format (see e.g. [Rieffel and Polak, 2011, Chapter 6]).



Figure 6. The shift circuits.

To use these shift components in the quantum circuit implementation of O_C , we need to control the applications of the L and R shift operators from the qubits that take $|\ell\rangle$ as the input. For $\ell = 0$, we need to apply the R -shift to account for

the -1 term in (4.14) and encode the row indices of the superdiagonal elements. For $\ell = 1$, nothing needs to be done. For $\ell = 2$, we need to apply the L -shift to account for the $+1$ term and encode the row indeces of the subdiagonal elements. Note that the use of D_s requires us to also consider $\ell = 3$ even though the matrix A only has 3 nonzero elements per column. In this case, we do not need to do anything. All of these conditions can be implemented by the following O_C circuit

$$\begin{array}{c} |\ell_1\rangle \\ |\ell_0\rangle \\ |j\rangle \end{array} \xrightarrow{O_C} = \begin{array}{c} \text{---} \\ \text{---} \\ \text{---} \end{array} \begin{array}{c} \text{---} \\ \text{---} \\ \text{---} \end{array} \begin{array}{c} \text{---} \\ \text{---} \\ \text{---} \end{array} \quad (4.16)$$

with the corresponding QCLAB code

```
QC = qclab.QCircuit(n+2,1);
QC.push_back(rightshift(n+2,2:n+1,[0,1],[0,0]));
QC.push_back(leftshift(n+2,2:n+1,[0,1],[1,0]));
```

We should note that the construction of O_C depends on how $c(j, \ell)$ is defined, which is not unique. For example, instead of defining $c(j, \ell)$ by (4.14), we can use the following definition

$$c(j, \ell) = \begin{cases} j & \text{if } \ell = 0 \text{ (diagonal) or } 3, \\ \text{mod}(j + 1, N) & \text{if } \ell = 1 \text{ (subdiagonal),} \\ \text{mod}(j - 1, N) & \text{if } \ell = 2 \text{ (superdiagonal),} \end{cases} \quad (4.17)$$

resulting in the O_C circuit

$$\begin{array}{c} |\ell_1\rangle \\ |\ell_0\rangle \\ |j\rangle \end{array} \xrightarrow{O_C} = \begin{array}{c} \text{---} \\ \text{---} \\ \text{---} \end{array} \begin{array}{c} \text{---} \\ \text{---} \\ \text{---} \end{array} = \begin{array}{c} \text{---} \\ \text{---} \\ \text{---} \end{array} \quad (4.18)$$

that can further be simplified because the L -shift and R -shift cancel each other for $\ell = 0$ and $\ell = 3$. The corresponding QCLAB code is given by

```
QC = qclab.QCircuit(n+2,1);
QC.push_back(leftshift(n+2,2:n+1,1));
QC.push_back(rightshift(n+2,2:n+1,0));
```

4.2.2 The O_A circuit

For circulant matrices, the matrix elements of A depend exclusively on ℓ . Therefore, when we use controlled rotations to encode the nonzero matrix elements, we place controls only on qubits that take $|\ell\rangle$ as the input. If $c(j, \ell)$ is defined by (4.17), the follow O_A circuit can be constructed to use the rotation $R_y(\theta_0)$ to encode the diagonal entry α . The rotation is applied when $\ell = 0$. The rotations $R_y(\theta_1)$ and $R_y(\theta_2)$ are used to encode the sub- and sup-diagonal matrix elements β and γ respectively. They are applied when $\ell = 1$ and $\ell = 2$ respectively.

$$\begin{array}{c} |0\rangle \\ |\ell_1\rangle \\ |\ell_0\rangle \\ |j\rangle \end{array} \xrightarrow{O_A} = \begin{array}{c} \text{---} \\ \text{---} \\ \text{---} \\ \text{---} \end{array} \begin{array}{c} R_y(\theta_0) \\ R_y(\theta_1) \\ R_y(\theta_2) \end{array} \begin{array}{c} \text{---} \\ \text{---} \\ \text{---} \\ \text{---} \end{array} \quad (4.19)$$

The unitary matrix implemented by the circuit can be written as

$$O_A =: O_A^{(2)} O_A^{(1)} O_A^{(0)}, \quad (4.20)$$

where

$$O_A^{(0)} = R_y(\theta_0) \otimes (E_0 \otimes E_0) \otimes I_n + I_2 \otimes (I_4 - E_0 \otimes E_0) \otimes I_n, \quad (4.21)$$

$$O_A^{(1)} = R_y(\theta_1) \otimes (E_0 \otimes E_1) \otimes I_n + I_2 \otimes (I_4 - E_0 \otimes E_1) \otimes I_n, \quad (4.22)$$

$$O_A^{(2)} = R_y(\theta_2) \otimes (E_1 \otimes E_0) \otimes I_n + I_2 \otimes (I_4 - E_1 \otimes E_0) \otimes I_n. \quad (4.23)$$

To determine the value of the rotation angle θ_0 from α , we first compute the quantum state after applying the diffusion operator $D_s = H \otimes H$, the $O_A^{(0)}$ circuit, and the O_C circuit to the initial state $|0\rangle|00\rangle|j\rangle$, i.e.,

$$\begin{aligned}
 & (I_2 \otimes O_C) O_A^{(0)} (I_2 \otimes D_s \otimes I_n) |0\rangle|00\rangle|j\rangle \\
 &= \frac{1}{2} (I_2 \otimes O_C) O_A^{(0)} |0\rangle (|00\rangle + |01\rangle + |10\rangle + |11\rangle) |j\rangle, \\
 &= \frac{1}{2} (I_2 \otimes O_C) (R_y(\theta_0) |0\rangle|00\rangle + |0\rangle|01\rangle + |0\rangle|10\rangle + |0\rangle|11\rangle) |j\rangle, \\
 &= \frac{1}{2} (R_y(\theta_0) |0\rangle|00\rangle|j\rangle + |0\rangle|01\rangle|j+1\rangle + |0\rangle|10\rangle|j-1\rangle + |0\rangle|11\rangle|j\rangle). \tag{4.24}
 \end{aligned}$$

Next, taking the inner product of (4.24) with $(I_2 \otimes D_s \otimes I_n) |0\rangle|00\rangle|j\rangle$ results in

$$\frac{1}{4} \langle j | \langle 00 | \langle 0 | R_y(\theta_0) | 0 \rangle | 00 \rangle | j \rangle + \frac{1}{4} \langle j | \langle 11 | \langle 0 | 0 \rangle | 11 \rangle | j \rangle = \frac{1}{4} [\cos(\frac{\theta_0}{2}) + 1], \tag{4.25}$$

where we use the fact that $\langle 0 | R_y(\theta_0) | 0 \rangle = \cos(\frac{\theta_0}{2})$. Finally, to satisfy the equality $\frac{1}{4} [\cos(\frac{\theta_0}{2}) + 1] = \frac{\alpha}{4}$, we obtain $\theta_0 = 2 \arccos(\alpha - 1)$. Without loss of generality, we have assumed α is real and positive. The case for $\alpha < 0$ can be handled by first multiplying A by -1 .

To calculate the rotation angle θ_1 from the subdiagonal element β , we start again from the quantum state after applying D_s , $O_A^{(1)}$, and O_C to $(I_2 \otimes D_s \otimes I_n) |0\rangle|00\rangle|j\rangle$, i.e.,

$$\begin{aligned}
 & (I_2 \otimes O_C) O_A^{(1)} (I_2 \otimes D_s \otimes I_n) |0\rangle|00\rangle|j\rangle \\
 &= \frac{1}{2} (I_2 \otimes O_C) O_A^{(1)} |0\rangle (|00\rangle + |01\rangle + |10\rangle + |11\rangle) |j\rangle, \\
 &= \frac{1}{2} (I_2 \otimes O_C) (|0\rangle|00\rangle + R_y(\theta_1) |0\rangle|01\rangle + |0\rangle|10\rangle + |0\rangle|11\rangle) |j\rangle, \\
 &= \frac{1}{2} (|0\rangle|00\rangle|j\rangle + R_y(\theta_1) |0\rangle|01\rangle|j+1\rangle + |0\rangle|10\rangle|j-1\rangle + |0\rangle|11\rangle|j\rangle). \tag{4.26}
 \end{aligned}$$

Next, taking the inner product of (4.26) with $(I_2 \otimes D_s \otimes I_n) |0\rangle|00\rangle|j+1\rangle$ results in

$$\frac{1}{4} \langle j+1 | \langle 01 | \langle 0 | R_y(\theta_1) | 0 \rangle | 01 \rangle | j+1 \rangle = \frac{1}{4} \cos(\frac{\theta_1}{2}), \tag{4.27}$$

where we use the fact that $\langle 0 | R_y(\theta_1) | 0 \rangle = \cos(\frac{\theta_1}{2})$. Finally, to satisfy the equality $\frac{1}{4} \cos(\frac{\theta_1}{2}) = \frac{\beta}{4}$, we obtain $\theta_1 = 2 \arccos(\beta)$.

In a similar way, we can show that $\theta_2 = 2 \arccos(\gamma)$. The O_A circuit (4.19) corresponding to the O_C circuit (4.18) can be implemented in QCLAB as

```

theta0 = 2*acos(alpha - 1);
theta1 = 2*acos(beta);
theta2 = 2*acos(gamma);
OA = qclab.QCircuit(n+3);
OA.push_back(qclab.qgates.MCRotationY([1,2],0,[0,0],theta0));
OA.push_back(qclab.qgates.MCRotationY([1,2],0,[0,1],theta1));
OA.push_back(qclab.qgates.MCRotationY([1,2],0,[1,0],theta2));

```

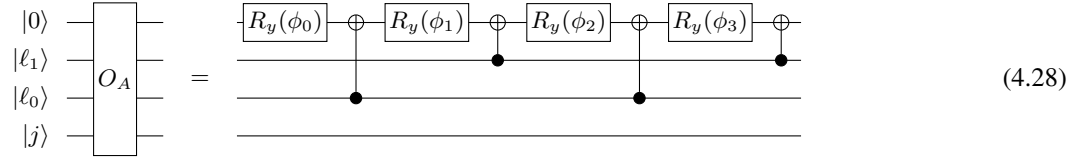
If we choose to use (4.14) to define $c(j, \ell)$, we can use controlled rotations by $R_y(\theta_0)$, $R_y(\theta_1)$ and $R_y(\theta_2)$ to encode γ , α and β respectively. It can be shown that corresponding rotations angles are $\theta_0 = 2 \arccos(\gamma)$, $\theta_1 = 2 \arccos(\alpha - 1)$, and $\theta_2 = 2 \arccos(\beta)$. The Q_A circuit can be implemented in QCLAB as

```

theta0 = 2*acos(gamma);
theta1 = 2*acos(alpha - 1);
theta2 = 2*acos(beta);
OA = qclab.QCircuit(n+3);
OA.push_back(qclab.qgates.MCRotationY([1,2],0,[0,0],theta0));
OA.push_back(qclab.qgates.MCRotationY([1,2],0,[0,1],theta1));
OA.push_back(qclab.qgates.MCRotationY([1,2],0,[1,0],theta2));

```

In both cases, we can again replace multi-qubit controlled R_y rotations in (4.19) with a uniformly controlled rotation. This approach leads to an O_A circuit that has the following structure



which we implement in QCLAB as follows

```
OA = qclab.QCircuit(n+3);
OA.push_back(ucry([theta_0,theta_1,theta_2]));
```

The angles ϕ_i are computed from θ_i through a Walsh-Hadamard transformation Möttönen et al. [2004].

4.2.3 The complete circuit

The complete circuit for a block encoding of $A/4$ for a 8×8 circulant matrix of the form (4.13) is given in fig. 7. The total number of Hadamard gates and controlled rotations are proportional to $\log(s)$ which is generally very small for a sparse matrix. The number of controlled R and L shifts is also on the order of $O(\log s)$. Each controlled- R and controlled- L circuit is a general multi-qubit controlled (Toffoli) gate that can be further decomposed into $\text{poly}(n)$ two-qubit gates. Therefore, the overall gate complexity of the U_A circuit is $\text{poly}(n)$, which is considered efficient.

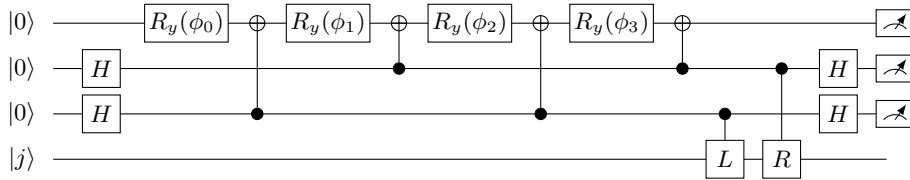


Figure 7. A complete quantum circuit for the block encoding of a 8×8 banded circulant matrix.

We should also note that the circuit shown in fig. 7 can be easily modified to block encode a tridiagonal matrix with α on the diagonal, β on the subdiagonal and γ on the superdiagonal. All we need to do is to add the following two multi-qubit control gates to the sequence of gates in the O_A block of the circuit. These gates perform controlled rotations $R_y(\pi - \theta_1)$ and $R_y(\pi - \theta_2)$ to zero out β in the $(0, N - 1)$ th entry of U_A and γ in the $(N - 1, 0)$ th entry of U_A , respectively, as shown in Figure 8.

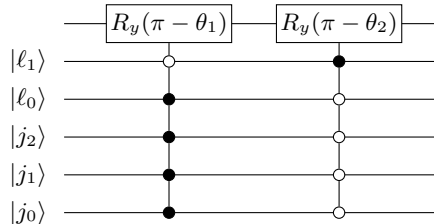
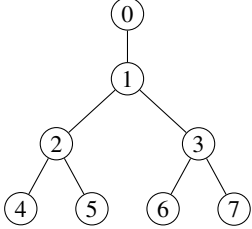


Figure 8. Multi-qubit controlled rotations that can be added to the quantum circuit shown in fig. 7 between O_A and O_C to block encode a tri-diagonal matrix.

4.3 Extended binary tree

The banded circulant matrix is special in the sense that the $c(j, \ell)$ function is relatively simple, and the values of nonzero matrix elements are independent of j . Next we consider another special case that has a slightly more complicated $c(j, \ell)$ function. In this case, the matrix A is the adjacency matrix for an undirected and balanced binary tree. A standard balanced binary tree has $2^n - 1$ vertices. To simplify our discussion, we add one additional vertex and connect it to the root of the binary tree so that the total number of vertices is 2^n . The additional vertex is the new root of the tree and

labeled by 0. We call this binary tree an extended binary tree and consider the following extended binary tree with 8 vertices and associated 8×8 adjacency matrix



$$A = \begin{bmatrix} \gamma & \beta & & & & & & \\ \beta & \alpha & \beta & \beta & & & & \\ \beta & \alpha & \alpha & \beta & \beta & & & \\ \beta & & \alpha & \beta & \beta & \beta & & \\ \beta & & \beta & \gamma & \gamma & & \beta & \\ \beta & & \beta & & \gamma & & \beta & \\ \beta & & \beta & & & \gamma & & \\ \beta & & \beta & & & & \gamma & \end{bmatrix}. \quad (4.29)$$

We assign the weight $0 < \alpha < 1$ to each vertex (or self loop from a vertex to itself) with the exception of the root and leaves of the tree. For those vertices, we assign the weight $0 < \gamma < 1$ instead. We assign the weight $0 < \beta < 1$ to each edge between a parent and its child.

4.3.1 The O_C circuit

The function $c(j, \ell)$ associated with the nonzero pattern of the adjacency matrix (4.29) can be defined as

$$c(j, \ell) = \begin{cases} 2j & \text{if } \ell = 0 \text{ (left child),} \\ 2j + 1 & \text{if } \ell = 1 \text{ (right child),} \\ j/2 & \text{if } \ell = 2 \text{ and } j \text{ even (parent),} \\ (j-1)/2 & \text{if } \ell = 3 \text{ and } j \text{ odd (parent),} \\ j & \text{if } \ell = 4 \text{ (diagonal).} \end{cases} \quad (4.30)$$

Because this function involves multiplying a column index j by 2 and dividing j by 2, the O_C circuit will contain controlled subcircuits that perform these operations in addition to the controlled L -shift and R -shift circuits used to perform the addition and subtraction by 1 for $\ell = 1$ and $\ell = 3$, respectively.

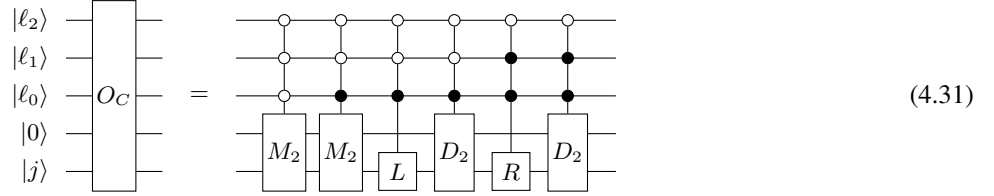
The mapping from $|j\rangle$ to $|2j\rangle$ can be defined by a unitary operator M_2 which consists of a sequence of swap operations between adjacency qubits as shown in fig. 9a. Note that the bottom 3 qubits are used to encode the column index with $|j_0\rangle$ being the label for the least significant and $|j_2\rangle$ being the label for the most significant bits. The top qubit labelled by $|0\rangle$ is an ancilla qubit that serves as a carry for $j \geq 4$.



Figure 9. The quantum circuits for (a) multiplying $|j\rangle$ by 2 and (b) dividing $|j\rangle$ by 2.

The mapping from $|j\rangle$ to $|j/2\rangle$, which we denote by D_2 , is the inverse operation of M_2 . Thus, we can simply reverse the sequence of SWAP gates in fig. 9a to obtain a circuit for D_2 in fig. 9b. Note that in this case, the least significant $|j_0\rangle$ ends up at the top qubit after D_2 is applied. This is problematic because taking the inner product of $D_2(|0\rangle |j\rangle)$ with $|0\rangle |i\rangle$, which appears in the evaluation of the (i, j) th element of U_A , will always result in 0, which means that we cannot properly encode the non-zero element $A_{i,j}$ when i is the parent of j and j is odd. However, this problem can be resolved by subtracting 1 from $|j\rangle$, if j is odd, before applying D_2 to ensure that a $|0\rangle$ state is always present on the ancilla qubit after O_C is applied.

With properly constructed M_2 and D_2 circuits, we can implement the O_C circuit as follows



with the corresponding QCLAB code

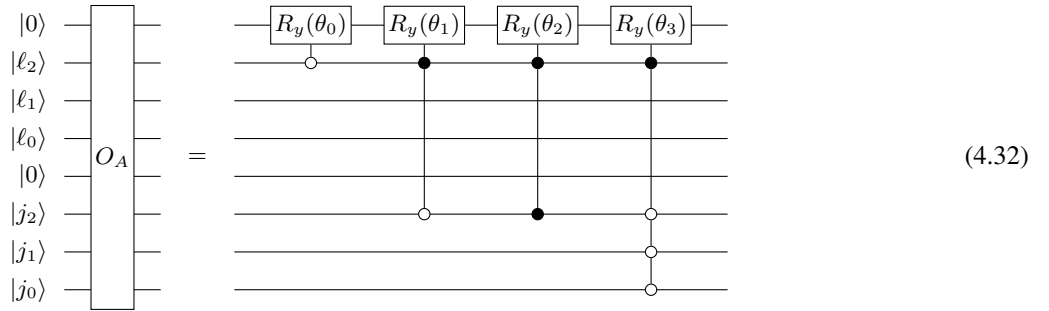
```
OC = qclab.QCircuit(n+4,1);
OC.push_back(    mul2(n+4,3:n+3,[0,1,2],[0,0,0]));
OC.push_back(    mul2(n+4,3:n+3,[0,1,2],[0,0,1]));
OC.push_back(  leftshift(n+4,4:n+3,[0,1,2],[0,0,1]));
OC.push_back(    div2(n+4,3:n+3,[0,1,2],[0,1,0]));
OC.push_back(rightshift(n+4,4:n+3,[0,1,2],[0,1,1]));
OC.push_back(    div2(n+4,3:n+3,[0,1,2],[0,1,1]));
```

4.3.2 The O_A circuit

As we indicated earlier, the construction of the O_A quantum circuit depends closely on how O_C is constructed. For the adjacency matrix associated with the extended binary tree, the O_A circuit corresponding to the O_C circuit shown in eq. (4.31) can be constructed as follows:

1. First, we use a rotation angle $\theta_0 = 2 \arccos(\beta)$ controlled by $\ell_2 = 0$ to place β on the off-diagonals of the principal leading block of U_A .
2. Second, we use a rotation angle $\theta_1 = 2 \arccos(\frac{\alpha}{4})$ controlled by $(\ell_2, j_2) = (1, 0)$ to place α at the diagonal elements not corresponding to the root or leaves.
3. Third, we use a rotation angle $\theta_2 = 2 \arccos(\frac{\gamma}{4})$ controlled by $(\ell_2, j_2) = (1, 1)$ to place γ at the diagonal elements corresponding to the leaves.
4. Finally, we use a rotation angle $\theta_3 = 2 \arccos(\frac{\gamma}{4} - \frac{\beta}{2}) - \theta_1$ controlled by $(\ell_2, j) = (1, 0)$ to fix the leading element of U_A .

The complete O_A circuit resulting from the above procedure can be implemented by the following circuit



with the corresponding QCLAB code

```
theta0 = 2*acos(beta);
theta1 = 2*acos(alpha/4);
theta2 = 2*acos(gamma/4);
theta3 = 2*acos(gamma/4 - beta/2) - theta1;
OA = qclab.QCircuit(n+5);
OA.push_back(qclab.qgates.CRotationY(1,0,theta0,0));
OA.push_back(qclab.qgates.MCRotationY([1,5],0,[1,0],theta1));
OA.push_back(qclab.qgates.MCRotationY([1,5],0,[1,1],theta2));
OA.push_back(qclab.qgates.MCRotationY([1,5:n+4],0,...[1,zeros(1,n)],theta3));
```

4.3.3 The complete circuit

Combining the O_C and O_A circuits, we obtain the complete circuit for the block encoding of the 8×8 adjacency matrix associated with the 8-vertex extended binary tree as shown in fig. 10.

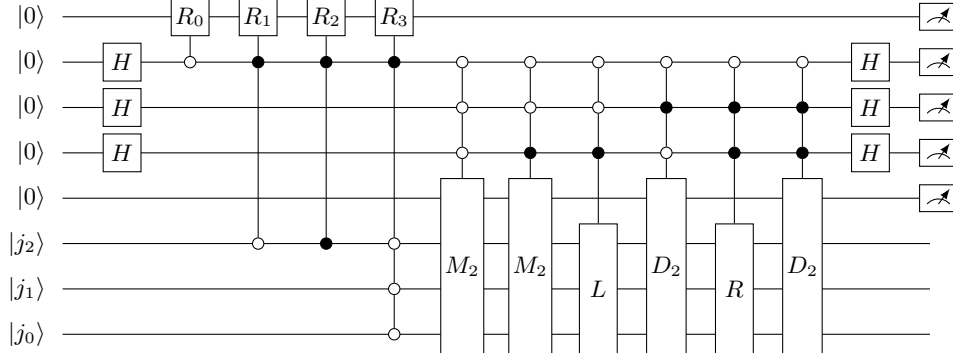


Figure 10. The full block-encoding quantum circuit for the adjacency matrix associated with the extended binary tree shown in eq. (4.29).

This circuit can be easily generalized for larger adjacency matrices associated with an extended binary tree with a larger number ($N = 2^n$) of vertices. However, because the number of unique cases defined by the function $c(j, \ell)$ in (4.30) is a constant 4 due to the relatively small number of additional vertices each vertex is connected to, the number of the controlled multiplication, division and additional gates in O_C is fixed. Furthermore, because the number of distinct values of matrix elements in A is fixed at 3, the number of controlled rotations required in O_A is also fixed. Each of these controlled rotations can be further decomposed into a subcircuit with $\mathcal{O}(\text{poly}(n))$ two-qubit gates. The overall gate complexity of the quantum circuit is $\mathcal{O}(\text{poly}(n))$, which is considered efficient.

5 Efficient circuits for the block encoding of a symmetric stochastic matrix and quantum walks

In the previous section, we presented a general technique for constructing an efficient quantum circuit to block encode A/s for a properly scaled s -sparse matrix A . For many applications such as solving a linear system, the $1/s$ factor does not fundamentally change the solution besides a simple rescaling (though a large scaling factor can reduce the final success probability). However, for other applications, introducing the $1/s$ factor is problematic. One such an application is the construction of a quantum walk from the block encoding of an s -sparse symmetric stochastic matrix P . For such a matrix, we need a different strategy to construct an efficient quantum circuit that block encodes P directly instead of P/s .

In this section, we will give a brief introduction of the construction of a quantum walk from the block encoding of a symmetric s -sparse stochastic matrix P associated with a classical random walk. We will explain why it is important to block encode P instead of P/s , and present a strategy for constructing an efficient quantum circuit for block encoding P . We will also show how such a circuit can be used to construct a quantum circuit for a quantum walk.

A stochastic matrix P , also called a Markov chain matrix, describes the transition probabilities of traversing from one vertex to another in a random walk on a graph $G = (V, E)$. Since the matrix element P_{ij} represents the probability of walking from vertex i to vertex j , it satisfies

$$P_{ij} \geq 0, \quad \sum_j P_{ij} = 1. \quad (5.1)$$

A stochastic matrix has many interesting properties, which are briefly summarized in the supplementary materials. In particular, it can be used to model a classical random walk, which can be characterized by the equation $w = P^k v$, where the i th element of the initial state v specifies the probability of a walker being at vertex i initially, and the i th element of the final state w gives the probability of the walker being at vertex i after k steps of random walks have been taken using P as the transition probability. The efficiency of the walk is often measured in terms of the number of steps it takes to reach a certain vertex (hitting time).

For a symmetric P , which becomes a doubly stochastic Markov chain matrix, and is what we consider later in this section, a more efficient type of walk, called *quantum walk* Mackay et al. [2002], Venegas-Andraca [2012] can be

constructed by block encoding $T_k(P)$, where $T_k(t) = \cos(k \arccos(t))$ is the k th degree Chebyshev polynomial of the first kind. When such a block encoding is applied to an initial state prepared as $|v\rangle|0\rangle$, it yields

$$w = (T_k(P)|v\rangle)|0\rangle + |*\rangle|1\rangle, \quad (5.2)$$

where $*$ denotes a vector that we do not care about. After measuring the second register and obtaining $|0\rangle$, the first register contains $T_k(P)|v\rangle$. This suggests that performing k steps of a quantum walk yields $T_k(P)|v\rangle$ instead of $P^k|v\rangle$. The consequence of such a transformation will be discussed in the supplementary materials through a specific application of a quantum walk.

Quantum walks have found many other applications in quantum algorithms Shenvi et al. [2003], Paparo and M. [2012]. In this section, we will present the block encoding view of a quantum walk and examine quantum circuits for the block encoding of $T_k(P)$, which is in turn expressed in terms of the block encoding of P .

5.1 Direct block encoding of P and $T_k(P)$

For an s -sparse P , we can use the techniques discussed in section 4 to construct an efficient quantum circuit that block encodes P/s .

Once we have the block encoding for P/s , we can use the QET discussed in section 3 to construct a quantum circuit for a block encoding of $T_k(P/s)$. However, our ultimate goal for implementing a quantum walk is not to have a block encoding of $T_k(P/s)$ but for $T_k(P)$ because P/s is not a stochastic matrix. To overcome this difficulty, we may express the k th degree Chebyshev polynomial $T_k(t)$ in terms of $T_j(t/s)$ for $j = 0, 1, \dots, k$, i.e.,

$$T_k(t) = \tilde{T}_k(t') = \sum_{j=0}^k \alpha_j T_j(t'), \quad (5.3)$$

where $t' = t/s$ and $\alpha_j = 0$ for odd (even) j if k is even (odd).

For example, when $s = 4$,

$$T_2(t) = \tilde{T}_2(t') = 15 + 16T_2(t'), \text{ where } t' = t/4. \quad (5.4)$$

We then try to use the QET to construct a block encoding of $\tilde{T}_k(t')$. However, to use the QET, the magnitude of the polynomial $\tilde{T}_k(t')$ must be bounded by 1 within the interval $[-1, 1]$. Since the magnitude of $\tilde{T}_k(t')$ can be much larger than 1 at $t' = \pm 1$, we need to scale $\tilde{T}_k(t')$ by $1/|\tilde{T}_k(1)|$ before using the QET. For example, for $s = 4$, $\tilde{T}_2(1) = 31$. As a result, we need to divide $\tilde{T}_2(t')$ in (5.4) by 31 before applying the QET. Consequently, we effectively construct a block encoding for $T_2(P)/\alpha$, where $\alpha = \tilde{T}_k(1)$, instead of $T_k(P)$. This has the effect of lowering the probability of successful measurement of $|0\rangle$ in (5.2) (when $T_k(P)$ is replaced with $T_k(P)/\alpha$.)

Nonetheless, we can construct a quantum circuit for such a block encoding. For $k = 2$, it follows from the discussion in section 3 and fig. 3 that such a circuit can be drawn as the one shown in fig. 11, where the phase angles

$$\phi_0 = 1.17, \phi_1 = 0.8, \phi_2 = 1.17$$

can be found numerically by using QSPPACK Dong et al. [2021] and $U_{P/s}$ denotes the block encoding of P/s .

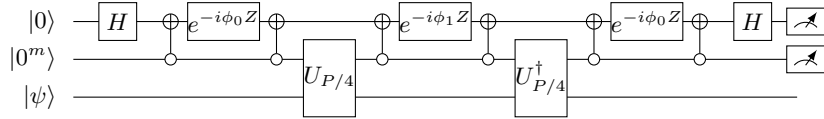


Figure 11. A quantum circuit for $T_2(P)/31$ for a sparse symmetric stochastic matrix P with at most 4 nonzero matrix elements per column using $U_{P/4}$ which is the block encoding for $P/4$.

5.2 An alternative block encoding scheme and its connection to a Szegedy's quantum walk

There is a way to block encode P instead of P/s . Such a block encoding scheme relies on using a different unitary oracle O_P that carries out the following mapping

$$O_P |0^n\rangle |j\rangle = \sum_k \sqrt{P_{jk}} |k\rangle |j\rangle. \quad (5.5)$$

Thanks to the stochasticity of P , the right hand side is already a normalized vector, and no additional ancilla qubit is needed.

The following theorem describes the structure of the blocking encoding constructed from a combination of O_P and an n -qubit swap operator that performs the following operation

$$\text{SWAP} |i\rangle |j\rangle = |j\rangle |i\rangle, \quad (5.6)$$

which swaps the value of the two registers in the computational basis, and can be directly implemented using n two-qubit SWAP gates.

Theorem 5.1. *If P is a symmetric stochastic Markov chain matrix, and if there exists a unitary operator O_P that can be used to carry out the mapping defined in Eq. (5.5), then*

$$U_P = O_P^\dagger \text{SWAP} O_P \quad (5.7)$$

is a Hermitian block encoding of P , where the swap operator SWAP is defined by Eq. (5.7).

Proof. Clearly U_P is unitary and Hermitian. Now we compute as before

$$|0^n\rangle |j\rangle \xrightarrow{O_P} \sum_k \sqrt{P_{jk}} |k\rangle |j\rangle \xrightarrow{\text{SWAP}} \sum_k \sqrt{P_{jk}} |j\rangle |k\rangle. \quad (5.8)$$

Meanwhile

$$|0^n\rangle |i\rangle \xrightarrow{O_P} \sum_{k'} \sqrt{P_{ik'}} |k'\rangle |i\rangle. \quad (5.9)$$

The inner product of (5.8) and (5.9) yields (using $P_{ij} = P_{ji}$)

$$\langle 0^n | \langle i | U_P | 0^n \rangle | j \rangle = \sum_{k,k'} \sqrt{P_{ik'} P_{jk}} \delta_{j,k'} \delta_{i,k} = \sqrt{P_{ij} P_{ji}} = P_{ij}. \quad (5.10)$$

□

Note the symmetry requirement for P in the above theorem is not essential. When $P \neq P^T$, we can work with the discriminant matrix defined in the supplementary materials. To simplify notation, we assume P is symmetric below. We should also note that in general the block encoding of a Hermitian matrix A is not necessarily Hermitian. theorem 5.1 gives a Hermitian block encoding of a Hermitian P , which is important for performing an efficient quantum walk. A more general approach of constructing a Hermitian block encoding of a Hermitian matrix A is discussed in the supplementary materials. However, the computational advantage of the Hermitian block encoding over a general block encoding of the same Hermitian matrix is still unclear at this stage.

We now discuss how to construct an efficient circuit for O_P using the banded circulant matrix (4.13) as an example, where we assume $\alpha + \beta + \gamma = 1$ for the matrix to be stochastic and $\beta = \gamma$. The construction of a block-encoding circuit can be done in two steps. In the first step, we construct a unitary K that performs the following mapping

$$K |0^n\rangle = (\sqrt{\alpha} \sqrt{\beta} 0 \cdots 0 \sqrt{\gamma})^T. \quad (5.11)$$

The first column of K has to encode the square root of the first column of the circulant matrix. It is generally possible to construct a circuit for performing such a unitary transformation using fully-controlled quantum Givens rotations that zero out elements in the vector in Gray code ordering Vartiainen et al. [2004]. Our approach is similar, but exploits the sparsity of (5.11) to further reduce the gate complexity to $\mathcal{O}(n)$ for this special case. The circuit for K , shown in fig. 12, is best explained in reverse order by considering the action of K^\dagger . The inverse operation for K^\dagger starts with a sequence of multi-controlled NOT gates that permute the non-zero element in the $N - 1$ st (last) row to row 3. We can now zero out $\sqrt{\gamma}$ in row 3 by applying the rotation $R_y(\theta_2)$ with $\theta_2 = -\arctan \sqrt{\frac{\gamma}{\beta}}$ to rows 1 and 3 of resulting state. Finally, we can zero out the element $\sqrt{\beta + \gamma}$ in row 1 of the resulting state against $\sqrt{\alpha}$ in row 0 with the rotation $R_y(\theta_1)$ where $\theta_1 = -\arctan \sqrt{\frac{\beta + \gamma}{\alpha}}$. To obtain a circuit for K , we reverse the order of operations listed above and negate the signs on the rotation angles as shown in Figure 12.

In the second step, we use the fact that $P e_j = L_n^{j-1} P e_0$, where e_j is the j th column of the identity matrix, to construct a controlled shift (adder) circuit to map $|P e_0\rangle |j\rangle$ to $|P e_j\rangle |j\rangle$. We show in the supplementary materials how such a controlled L -shift circuit is derived. Combining these two steps as well as the SWAP operator, we can represent the quantum circuit for the Hermitian block encoding of P by the diagram shown in fig. 13.

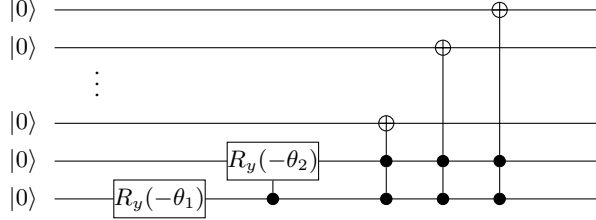


Figure 12. A quantum circuit for the state preparation unitary K given in (5.11).

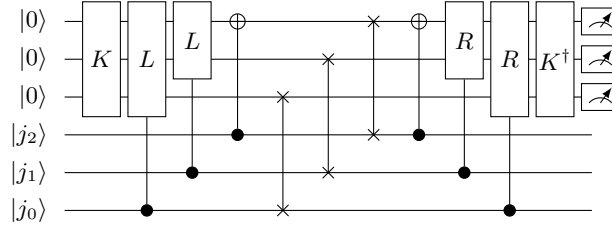


Figure 13. The complete quantum circuit for a Hermitian block encoding of the 8×8 Hermitian banded circulant matrix P defined by (4.13) with $\alpha > 0$, $\gamma = \beta > 0$ and $\alpha + 2\beta = 1.0$.

Once a quantum circuit for a symmetric block encoding of P is available, we can then use QET to construct a circuit that block encodes $T_k(P)$ for a k th degree of Chebyshev polynomial. It can be easily shown that the phase angles required in the QET circuit are

$$\varphi_0 = \pi/2, \varphi_1 = \dots = \varphi_{k-1} = \pi/2 \text{ and } \varphi_k = 0. \quad (5.12)$$

It follows from the discussion in section 3 that the circuit for the block encoding of $T_k(P)$ has a structure shown in fig. 14.

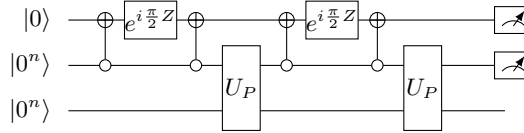


Figure 14. The overall structure of a quantum circuit for the block encoding of $T_2(P)$.

In the following, we draw the connection between the block encoding view of a quantum walk with early studies of quantum walks that are often written as the product of a swap operator and a reflector. Such a quantum walk are sometimes referred to as the *Szegedy quantum walk* Szegedy [2004]. We should note that there are alternative formulations of quantum walks and efficient methods for constructing quantum circuits for these formulations Lemieux et al. [2020].

We begin by noticing that the first two multi-qubit controlled NOT gates and the single qubit phase gate labelled by $e^{i\pi/2 Z}$ can be viewed as a way to implement the $e^{i\pi/2 Z_{\Pi}}$ operator, where Z_{Π} is a reflector defined as

$$Z_{\Pi} \equiv 2\Pi - I, \quad (5.13)$$

with $\Pi \equiv |0^n\rangle\langle 0^n| \otimes I_N$. In general, such a circuit block is used to implement $e^{i\phi Z_{\Pi}}$, which appears in the block encoding of a matrix polynomial, for an arbitrary angle ϕ . However, when $\phi = \pi/2$, we can use the identity $e^{i\pi/2 Z_{\Pi}} = -iZ_{\Pi}$ to simplify the block encoding circuit. This simplification allows us to rewrite the block encoding of $T_k(P)$ as (up to an irrelevant global phase factor $(-i)^k$)

$$U_{T_k(P)} = (U_P Z_{\Pi})^k. \quad (5.14)$$

Substituting the symmetric block encoding U_P defined in (5.7) into (5.14) and grouping O_P^{\dagger} , $Z_{\Pi} \otimes I$, O_P and SWAP together allows us to express $U_{T_k(P)}$ in terms of repeated applications of

$$\text{SWAP} \cdot U_R, \quad (5.15)$$

where $U_R \equiv O_P (Z_\Pi \otimes I) O_P^\dagger$ is a reflector. This indicates that the block encoding of $T_k(P)$ is equivalent to performing k steps of a Szegedy quantum walk, which is typically defined as the product of a reflection and a swap operator. We will show this equivalence more precisely in the supplementary materials.

It follows that constructing an efficient circuit for the Szegedy quantum walk is equivalent to constructing an efficient circuit for the symmetric block encoding of P defined in (5.7). We should note that a method for constructing efficient quantum circuits for a Szegedy quantum walk on structured graphs was previously presented in Loke and Wang [2017]. We now show that this method is equivalent to the construction of the block encoding circuit for P .

The method presented in Loke and Wang [2017] seeks a unitary transformation V in the form of $\sum_{i=0}^{N-1} V_i \otimes |i\rangle\langle i|$ to diagonalize U_R . If V_i 's can be found to satisfy $V_i |\phi_i\rangle = |b\rangle$ for a computational basis $|b\rangle$, then one can verify that

$$V^\dagger U_R V = 2 \sum_{i=0}^{N-1} (V_i^\dagger |\phi_i\rangle\langle\phi_i| V_i) \otimes |i\rangle\langle i| = 2(|b\rangle\langle b| - I). \quad (5.16)$$

If $|b\rangle$ is chosen to be $|0^n\rangle$, the right hand side of (5.16) becomes the Z_Π matrix appeared in (5.14).

The transformation V defined in (5.16) is equivalent to the O_P transformation defined by (5.5). Hence, constructing a circuit for O_P is equivalent to constructing a circuit for V . When this circuit is combined with the circuit implementation of Z_Π , we obtain a quantum circuit for the Szegedy quantum walk that is equivalent to the circuit presented in Loke and Wang [2017].

6 Concluding remarks

Block encodings and quantum eigenvalue/singular value transformations provide a powerful framework for solving large sparse linear algebra problems on quantum computers. However, to make this approach practical, we need to construct block encoding unitaries that can be easily decomposed into efficient quantum circuits. Although the general strategies for constructing such block encoding unitaries have been proposed in terms of oracles in the past, not much effort has been developed to the explicit construction of quantum circuits for realizing these block encodings.

Our work in this paper is focused on addressing this practical issue. In particular, we discussed techniques for constructing an efficient quantum circuit for the block encoding of an s -sparse matrix A/s and gave some specific examples. In general, the block encoding circuit consists of an O_c circuit block that encodes the nonzero structure of the matrix and an O_A circuit that encodes the numerical values of the nonzero matrix elements. Without an efficient implementation of these oracles with $\text{poly}(n)$ gate complexity, it can be very difficult to achieve exponential quantum advantage over classical algorithms Tang [2021], Gharibian and Gall [2021]. Through explicit examples, we show what is required to construct these circuit blocks and that the construction of these circuit blocks may not be completely independent of each other. In particular, the O_A circuit may be constructed to zero out certain matrix element to maintain the desired sparsity structure.

For a general sparse matrix A , constructing an efficient block encoding of A/s can be non-trivial. In particular, it may be difficult to find an efficient O_c if the sparsity pattern of A is somewhat arbitrary. In some cases, a more general block encoding scheme that includes an additional O_r unitary that encodes the row sparsity separately from the column sparsity may be needed.

The general construction procedure is not suitable for block encoding a sparse symmetric stochastic matrix P associated with a random walk on a graph when such a block encoding is used to implement a quantum walk on the same graph. For this type of matrices, an alternative construction procedure that yields a symmetric block encoding circuit for P instead of P/s is desired. Such a block encoding allows us to construct an efficient block encoding of a Chebyshev polynomial of P , which is the unitary used in a quantum walk. We showed that constructing a circuit for a block encoding of $T_k(P)$ is equivalent to a previously developed technique for constructing an efficient quantum circuit for Szegedy quantum walks on special graphs.

Throughout this paper, we assume that single qubit gates are available for an arbitrary rotation matrix, and that multi-qubit controls are available to carry out the required encoding schemes. No constraint has been placed on the topology of qubits and their connections. These assumptions certainly do not hold for existing quantum devices, and they are not expected to be valid for at least early fault-tolerant quantum computers. When the quantum gates available on these devices are restricted to a few elementary gates (such as Hadamard and Pauli gates), additional decompositions and transformations are required to express some of the gates (especially, the multi-qubit control gates) used in the block encoding circuits described above in terms of elementary gates. The circuit construction will also need to take the topology and connection of qubits into consideration. We will pursue efficient ways to construct this type of circuits in future works.

7 Appendix

7.1 Efficient circuits for powers of a shift operator

In section 4.2, we indicated that powers of a shift operator can be implemented efficiently without repeating the circuit associated with the shift operator. We will elaborate on this point a bit more in this section.

If we use L_n to denote an n -qubit L -shift operator of dimension $2^n \times 2^n$, then it can be shown that

$$L_n^2 = L_{n-1} \otimes I_2, \quad (7.1)$$

for $n > 1$. As a result, the circuit for the L_n^2 -shift operator can be drawn, for example, as in fig. 15 for $n = 3$. A similar decomposition holds for R_n^2 .



Figure 15. L^2 -shift circuit

Using the binary representation of an integer

$$j = [j_{n-1} \cdots j_1 j_0] = j_{n-1} \cdot 2^{n-1} + \cdots + j_1 \cdot 2^1 + j_0 \cdot 2^0,$$

for $j \in \mathbb{N} : 0 \leq j \leq 2^n - 1$, where $j_k \in \{0, 1\}$ for $0 \leq k \leq n - 1$, we can rewrite L^j as

$$L_n^j = \left(L_n^{2^{n-1}} \right)^{j_{n-1}} \cdot \left(L_n^{2^{n-2}} \right)^{j_{n-2}} \cdots \left(L_n^{2^0} \right)^{j_0}. \quad (7.2)$$

Applying (7.1) recursively to $L_n^{2^{n-k}}$ yields

$$L_n^{2^{n-k}} = L_k \otimes \underbrace{I_2 \otimes \cdots \otimes I_2}_{n-k}.$$

Therefore, to apply L_n^j to an input $|\ell\rangle$, we just need to apply a sequence of controlled L_k operations for $k = n, n-1, \dots, 1$ successively to the leading k qubits using $|j_k\rangle$ as the control for L_k as shown, for example, in fig. 16 for $n = 3$.

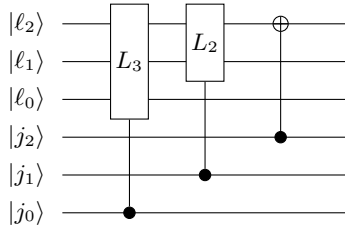


Figure 16. A quantum circuit for L_3^j .

7.2 Hermitian block encoding of Hermitian sparse matrices

In general, the block encoding unitary of a real symmetric or complex Hermitian matrix is not necessarily symmetric or Hermitian. This is clearly the case for the block encodings constructed in sections 4.2 and 4.3. It is also possible to obtain a Hermitian block encoding of a Hermitian matrix, which can simplify certain theoretical treatments (e.g. quantum walks). We will show how an efficient quantum circuit can be constructed for such a block encoding. The following theorem lays out the basic structure of such a circuit.

Theorem 7.1. Suppose A is a sparse Hermitian matrix of dimension 2^n with at most $s = 2^m$ non-zeros per column, with $m \leq n$. If a unitary O_C satisfies

$$O_C |\ell\rangle |j\rangle = |c(j, \ell)\rangle |j\rangle, \quad (7.3)$$

where $c(j, \ell)$ is the row index of the ℓ th non-zero elements in the j th column, and if there exists a unitary O_A such that

$$(I \otimes O_A) |0\rangle |0\rangle |i\rangle |j\rangle = |0\rangle \left(\sqrt{A_{ij}} |0\rangle + \sqrt{1 - |A_{ij}|} |1\rangle \right) |i\rangle |j\rangle. \quad (7.4)$$

For $A_{ij} = |A_{ij}|e^{i\theta_{ij}}, \theta_{ij} \in [0, 2\pi]$, the square root is uniquely defined as $\sqrt{A_{ij}} = \sqrt{|A_{ij}|}e^{i\theta_{ij}/2}$. Then the unitary U_A represented by the circuit shown in fig. 17 is a Hermitian block encoding of A , where D_s is a diffusion operator defined as

$$D_s \equiv I_2 \otimes \cdots \otimes \underbrace{H \otimes H \otimes \cdots H}_m,$$

and SWAP is a swap operator that swaps the last two n -qubit registers in fig. 17 respectively.

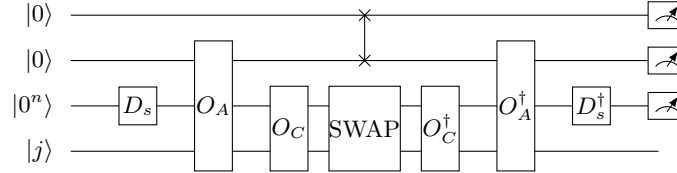


Figure 17. The general structure of a quantum circuit for a Hermitian block encoding of an s -sparse Hermitian matrix A . The S block represents a SWAP operator that swaps the the last two n -qubit registers qubit-by-qubit.

Proof. Our goal is to show that $\langle 0 | \langle 0 | \langle 0^n | \langle i | U_A | 0 \rangle | 0 \rangle | 0^n \rangle | j \rangle = A_{ij} / s$. In order to compute this inner product, we apply D_s, O_A, O_c to $|0\rangle |0\rangle |0^n\rangle |j\rangle$ successively as below

$$\begin{aligned} |0\rangle |0\rangle |0^n\rangle |j\rangle &\xrightarrow{D_s} \frac{1}{\sqrt{s}} \sum_{\ell \in [s]} |0\rangle |0\rangle |\ell\rangle |j\rangle \\ &\xrightarrow{O_A} \frac{1}{\sqrt{s}} \sum_{\ell \in [s]} |0\rangle \left(\sqrt{A_{c(j, \ell), j}} |0\rangle + \sqrt{1 - |A_{c(j, \ell), j}|} |1\rangle \right) |\ell\rangle |j\rangle \\ &\xrightarrow{O_c} \frac{1}{\sqrt{s}} \sum_{\ell \in [s]} |0\rangle \left(\sqrt{A_{c(j, \ell), j}} |0\rangle + \sqrt{1 - |A_{c(j, \ell), j}|} |1\rangle \right) |c(j, \ell)\rangle |j\rangle. \end{aligned} \quad (7.5)$$

After passing the SWAP gates, the state becomes

$$\frac{1}{\sqrt{s}} \sum_{\ell \in [s]} \left(\sqrt{A_{c(j, \ell), j}} |0\rangle + \sqrt{1 - |A_{c(j, \ell), j}|} |1\rangle \right) |0\rangle |j\rangle |c(j, \ell)\rangle. \quad (7.6)$$

We may similarly compute

$$\begin{aligned} |0\rangle |0\rangle |0^n\rangle |0\rangle |i\rangle &\xrightarrow{D_s} \xrightarrow{O_A} \xrightarrow{O_c} \\ &\frac{1}{\sqrt{s}} \sum_{\ell' \in [s]} |0\rangle \left(\sqrt{A_{c(i, \ell'), i}} |0\rangle + \sqrt{1 - |A_{c(i, \ell'), i}|} |1\rangle \right) |c(i, \ell')\rangle |i\rangle. \end{aligned} \quad (7.7)$$

Finally, taking the inner product between (7.6) and (7.7) yields

$$\begin{aligned} &\langle 0 | \langle 0 | \langle 0^n | \langle i | U_A | 0 \rangle | 0 \rangle | 0^n \rangle | j \rangle \\ &= \frac{1}{s} \sum_{\ell, \ell' \in [s]} \sqrt{A_{c(j, \ell), j}} \sqrt{A_{c(i, \ell'), i}^*} \delta_{i, c(j, \ell)} \delta_{c(i, \ell'), j} \\ &= \frac{1}{s} \sqrt{A_{ij} A_{ji}^*} \sum_{\ell, \ell'} \delta_{i, c(j, \ell)} \delta_{c(i, \ell'), j} = \frac{1}{s} A_{ij}. \end{aligned} \quad (7.8)$$

In this equality, we have used the fact that A is Hermitian: $A_{ij} = A_{ji}^*$, and there exists a unique ℓ such that $i = c(j, \ell)$, as well as a unique ℓ' such that $j = c(i, \ell')$. \square

We use the 8×8 banded circulant matrix defined by (4.13) with $0 < \alpha, \beta < 1, \beta = \gamma$ as an example to illustrate how to construct an efficient quantum circuit for a Hermitian block encoding of a Hermitian sparse matrix.

For this example, we define $c(j, \ell)$ to be used in the construction of the O_C circuit as

$$c(j, \ell) = \text{mod}(\ell + j - 1, N), \quad (7.9)$$

to represent the row index of the ℓ th non-zero matrix elements in the j th column. It is important to note that the definition of O_C in (7.3) is different from the definition given in (4.2). In (4.2), the qubit register that takes $|j\rangle$ as the input is changed and the register used to hold $|\ell\rangle$ is simply used as a control and is not altered after the unitary transformation. In (7.3), the register that holds $|\ell\rangle$ is changed while $|j\rangle$ is unchanged. Therefore, we need to construct a circuit that adds $j - 1$ to ℓ using $|j\rangle$ as the control. The addition of j to a quantum state can be carried by applying L^j to that state using the efficient circuit presented in the previous section.

The construction of the O_A circuit in this example is similar to the way O_A is constructed in section 4.2. We use rotations controlled by ℓ to place non-zero $\sqrt{A_{ij}}$ at appropriate locations in the principal leading block of U_A . To be specific, we use the rotation $R(\theta_1)$ with the angle $\theta_1 = \arccos(\sqrt{\beta} - 1)$ conditioned on $\ell = 0$ to place β on the supdiagonal. We use the rotation $R(\theta_2)$ with $\theta_2 = \arccos(\sqrt{\alpha}) + \pi$ conditioned on $\ell = 1$ to place α on the diagonal, and the rotation $R(\theta_3)$ with $\theta_3 = \arccos(\beta) + \pi$ to place β on the subdiagonal.

The complete circuit for the Hermitian block encoding of A is shown in fig. 18.

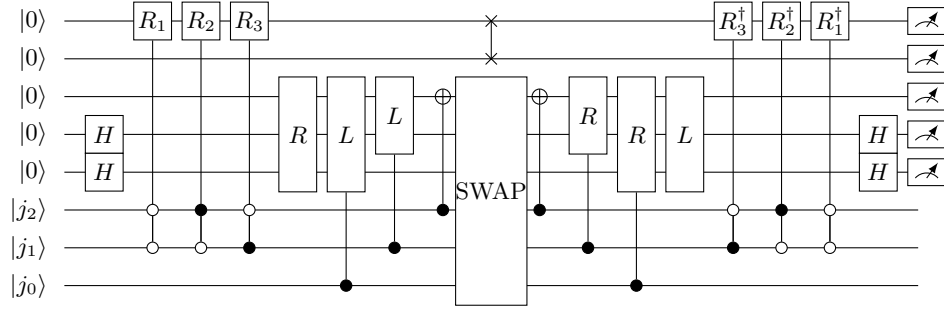


Figure 18. The complete quantum circuit for a Hermitian block encoding of the 8×8 Hermitian banded circulant matrix A defined by (4.13). The SWAP operator swaps the last two n -qubit registers qubit-by-qubit.

7.3 Additional results on quantum walks

In the following section, we provide additional materials that describe properties of a random walk as well as an application that demonstrates the higher (query) efficiency of a quantum walk compared to that of a classical random walk from a block encoding point of view.

7.3.1 Properties a Markov chain matrix

Because the sum of all probabilities of transitions from the vertex i to other vertices must be 1 for all i , the vector $(1 \ 1 \ \dots \ 1)^T$ is a right eigenvector of the Markov chain stochastic matrix P associated with the eigenvalue 1. The corresponding left eigenvector π is called a *stationary state* and satisfies

$$\pi^T P = \pi, \quad \pi_i \geq 0, \quad \sum_i \pi_i = 1. \quad (7.10)$$

A Markov chain matrix P is *irreducible* if any state can be reached from any other state in a finite number of steps of a random walk, i.e., the j th element of $w = P^k e_i$ is nonzero for any j and some finite k where e_i is the i th column of the identity matrix. An irreducible Markov chain is *aperiodic* if there exists no integer greater than one that divides the length of every directed cycle of the graph. A Markov chain is *ergodic* if it is both irreducible and aperiodic. By the Perron–Frobenius Theorem, any ergodic Markov chain P has a unique stationary state π in (7.10). A Markov chain is *reversible* if the following detailed balance condition is satisfied

$$\pi_i P_{ij} = \pi_j P_{ji}. \quad (7.11)$$

For a nonsymmetric but reversible P , we can construct a quantum walk by block encoding the *discriminant matrix* D associated with P . Such a matrix is defined componentwise as

$$D_{ij} = \sqrt{P_{ij}P_{ji}}, \quad (7.12)$$

which is real symmetric.

When P is reversible, it can be shown that

$$|\pi\rangle = \sum_i \sqrt{\pi_i} |i\rangle \quad (7.13)$$

is a normalized eigenvector of the discriminant matrix D defined by (7.12), i.e., $|\pi\rangle$ satisfies

$$D|\pi\rangle = |\pi\rangle. \quad (7.14)$$

Furthermore, because $\pi_i > 0$ for all i , we have

$$D = \text{diag}(\sqrt{\pi})P \text{diag}(\sqrt{\pi})^{-1}. \quad (7.15)$$

Therefore, for a reversible P , P and D share the same set of eigenvalues, and the spectral properties of a nonsymmetric P can be analyzed by working with the symmetric D matrix.

7.3.2 The equivalence of Szegedy quantum walk and block encoding of $T_k(D)$

The Szegedy quantum walk is traditionally introduced as follows. Using the following O_P oracle and the multi-qubit SWAP gate, we can define two set of quantum states

$$\begin{aligned} |\psi_j^1\rangle &= O_P |0^n\rangle |j\rangle = \sum_k \sqrt{P_{jk}} |k\rangle |j\rangle, \\ |\psi_j^2\rangle &= \text{SWAP}(O_P |0^n\rangle |j\rangle) = \sum_k \sqrt{P_{jk}} |j\rangle |k\rangle. \end{aligned} \quad (7.16)$$

These quantum states yield two projection operators

$$\Pi_l = \sum_{j \in [N]} |\psi_j^l\rangle \langle \psi_j^l|, \quad l = 1, 2, \quad (7.17)$$

from which we can define two $2n$ -qubit reflection operators $R_{\Pi_l} = 2\Pi_l - I_{2n}$. Let us write down the reflection operators more explicitly. Using the resolution of identity, we obtain

$$R_{\Pi_1} = O_P((2|0^n\rangle \langle 0^n| - I) \otimes I_n)O_P^\dagger = O_P(Z_\Pi \otimes I_n)O_P^\dagger, \quad (7.18)$$

where Z_Π is as defined in (5.13). Similarly, we have

$$R_{\Pi_2} = \text{SWAP } O_P(Z_\Pi \otimes I_n)O_P^\dagger \text{SWAP}. \quad (7.19)$$

Then Szegedy's quantum walk operator takes the form

$$\mathcal{U}_Z = R_{\Pi_2}R_{\Pi_1}, \quad (7.20)$$

which is a rotation operator that resembles the one that appears in the Grover's algorithm. Note that

$$\mathcal{U}_Z = \text{SWAP } O_P(Z_\Pi \otimes I_n)O_P^\dagger \text{SWAP } O_P(Z_\Pi \otimes I_n)O_P^\dagger, \quad (7.21)$$

so $O_P^\dagger \mathcal{U}_Z (O_P^\dagger)^{-1}$ is the same as a block encoding of $T_2(D)$ using qubitization up to a matrix similarity transformation. More generally, k -steps of Szegedy's quantum walk given by \mathcal{U}_Z^k is equivalent to a block encoding of $T_{2k}(D)$.

7.3.3 Quantum walk efficiency in detecting a marked vertex

In this section, we provide a brief explanation of the advantage of a quantum walk over a classical random walk from a block encoding point of view, i.e., why it is of interest to block encode $T_k(D)$ and perform the corresponding unitary transformation (5.2) on a quantum computer rather than simply applying P^k to an initial vector of probability distributions on a classical computer.

The direct consequence of applying $T_k(P)$ in a quantum walk (instead of P^k in a classical random walk) to v can be analyzed as follows. Since an eigenvalue λ of P is between -1 and 1 , we can reparameterize it as $\lambda = \cos \theta$. Clearly,

the corresponding eigenvalue of P^k is $\cos^k \theta$, and the corresponding eigenvalue of $T_k(P)$ is $\cos(k\theta)$. For small θ , it follows from the Taylor expansion of $\cos^k \theta$ and $\cos \hat{k}\theta$ that

$$\cos^k \theta = 1 - \frac{k\theta^2}{2} + O(k^2\theta^4), \quad (7.22)$$

$$\cos \hat{k}\theta = 1 - \frac{\hat{k}^2\theta^2}{2} + O(\hat{k}^4\theta^4), \quad (7.23)$$

for integers k and \hat{k} .

We can readily see that the Taylor expansions of these functions agree up to the second order term when $\hat{k} = \sqrt{k}$. This observation suggests that, for a reversible random walk, the second largest eigenvalue of $T_{\hat{k}}(P)$ can reach that of P^k when $\hat{k} = O(\sqrt{k})$. Since properties of a random walk is often determined by the gap between the largest eigenvalue and the second largest eigenvalue, this observation highlights the fundamental reason why a quantum walk can be asymptotically much faster than a classical random walk.

To demonstrate how a quantum walk can be used to solve a practical problem, let us examine the following example. Our goal is to detect the presence of a marked vertex in a graph $G = (V, E)$. Our assumption is that we do not know a priori whether such a marked vertex exists. Nor do we know the location of this vertex if it indeed exists. What we are given are some tools we can use to find out the presence of the marked vertex and its position if it is present.

In the classical setting, the tool we are given is a random walk transition probability matrix P (constructed by someone who knows the answer). We are allowed to apply P to a vector and check the result (but not allowed to look at P itself). The vector we will apply P to is prepared as $v = e/N$, where $e = (1, \dots, 1)^T$. It describes an initial uniform probability of being at any vertex. We examine the probability of being at each vertex after performing several steps of the random walk, i.e., we examine elements of the vector $w = P^k v$. If G contains a marked vertex, the element of w associated with such vertex will have a much higher magnitude. The position of this element informs us the position of the marked vertex.

To clearly demonstrate the advantage of performing a quantum walk, we choose G to be a complete graph, even though the efficiency of a quantum walk holds for a general graph. If no marked vertex is present in G , the matrix P we are given is

$$P = \frac{1}{N}ee^T, \quad e = (1, \dots, 1)^T. \quad (7.24)$$

Otherwise, if a marked vertex is present, and if, without loss of generality, the marked vertex is the 0-th vertex (which we do not know in advance), the matrix P we are given is

$$P = \begin{pmatrix} 1 & 0 \\ \frac{1}{N}\tilde{e} & \frac{1}{N}\tilde{e}\tilde{e}^T \end{pmatrix}, \quad (7.25)$$

where \tilde{e} is a vector of all ones of length $N - 1$.

Clearly, applying the P matrix defined by (7.24) to v does not change v . The output from such a random walk remains the same, i.e., the probability of being at each vertex remains at $1/N$.

However, if we are given the P matrix defined by (7.25), one can show that $w = P^k v$ converges to the eigenvector $\tilde{\pi} = (1, 0, \dots, 0)^T$ associated with the largest eigenvalue 1 of P when $k = \mathcal{O}(N)$. Hence, after performing $\mathcal{O}(N)$ steps of the random walk using this P , we can conclude, with high confidence, that there is a marked vertex and it is the 0th vertex since the 0th element of w is nearly 1.

In the quantum setting, the tool we are given is different. Instead of the P matrix, we are given the block encoding of the discriminant matrix D associated with P denoted by U_D . Again, we are allowed to apply U_D^k to a carefully prepared quantum state $|\psi_0\rangle$ to perform a quantum walk (but not allowed to look at U_D itself). The prepared initial quantum state is

$$|\psi_0\rangle = |0^n\rangle (H^{\otimes n} |0^n\rangle). \quad (7.26)$$

To detect the presence of a marked vertex, which is equivalent to determining whether the quantum walk operator is the block encoding of the discriminant matrix associated with the P matrix defined in (7.24) or (7.25), we measure the first n qubits, and evaluate the success probability of measuring the $|0^n\rangle$ state. This probability should be

$$p(|0^n\rangle) = \|(|0^n\rangle \langle 0^n| \otimes I_n)U_D^k |\psi_0\rangle\|^2. \quad (7.27)$$

Then, if U_D were the block encoding of P (which is the same as the corresponding discriminant matrix D when $P = P^T$), $U_D |\psi_0\rangle = |\psi_0\rangle$. As a result, the probability of measuring $|0^n\rangle$ is $p(|0^n\rangle) = 1$, regardless how many steps of the quantum walk are taken.

On the other hand, if U_D results from the block encoding of the discriminant matrix D associated with the P matrix defined in (7.25), which has the form

$$D = \begin{pmatrix} 1 & 0 \\ 0 & \frac{1}{N}\tilde{e}\tilde{e}^T \end{pmatrix}, \quad (7.28)$$

the success probability of measuring $|0^n\rangle$ can be much less than 1.

To see this, we recognize that the matrix D defined in (7.28) has two nonzero eigenvalues 1 and $(N-1)/N = 1 - \delta$, with the corresponding eigenvectors $|\tilde{\pi}\rangle = (1, 0, \dots, 0)^T$ and $|\tilde{v}\rangle = \frac{1}{\sqrt{N-1}}(0, 1, 1, \dots, 1)^T$, respectively. Because

$$|\psi_0\rangle = \frac{1}{\sqrt{N}}|0^n\rangle|\tilde{\pi}\rangle + \sqrt{\frac{N-1}{N}}|0^n\rangle|\tilde{v}\rangle, \quad (7.29)$$

it follows from the fact that U_D^k block encodes $T_k(D)$ that

$$U_D^k|\psi_0\rangle = \frac{1}{\sqrt{N}}|0^n\rangle T_k(1)|\tilde{\pi}\rangle + \sqrt{\frac{N-1}{N}}|0^n\rangle T_k(1-\delta)|\tilde{v}\rangle + |\perp\rangle, \quad (7.30)$$

where $|\perp\rangle$ is an unnormalized state satisfying $(|0^n\rangle\langle 0^n|) \otimes I_n|\perp\rangle = 0$. Since $T_k(1) = 1$ for all k , we have

$$p(0^n) = \frac{1}{N} + \left(1 - \frac{1}{N}\right)T_k^2(1-\delta). \quad (7.31)$$

Using the fact that $T_k(1-\delta) = \cos(k \arccos(1-\delta))$, we can show that $T_k(1-\delta) \approx 0$ when k satisfies

$$k \approx \frac{\pi}{2 \arccos(1-\delta)} \approx \frac{\pi}{2\sqrt{2\delta}} = \frac{\pi\sqrt{N}}{2\sqrt{2}}. \quad (7.32)$$

Therefore, after taking $k = \lceil \frac{\pi\sqrt{N}}{2\sqrt{2}} \rceil$ steps of the quantum walk, the probability of successfully measuring $|0^n\rangle$ drops down to $1/N$, which is significantly lower than 1. This will allow us to declare, with high confidence, the presence of a marked vertex in the graph in $\mathcal{O}(\sqrt{N})$ steps of a quantum walk, which is a significant (quadratic) speed up compared to $\mathcal{O}(N)$ steps of a random walk required in the classical setting for large N .

We simulate this experiment for $n = 6$ qubits in QCLAB. The script to reproduce this simulation is made available on <https://github.com/QuantumComputingLab/qclab>. We first generate quantum circuits that block encode the discriminant matrix for (7.24) and (7.25). These circuits are given in Figure 19.

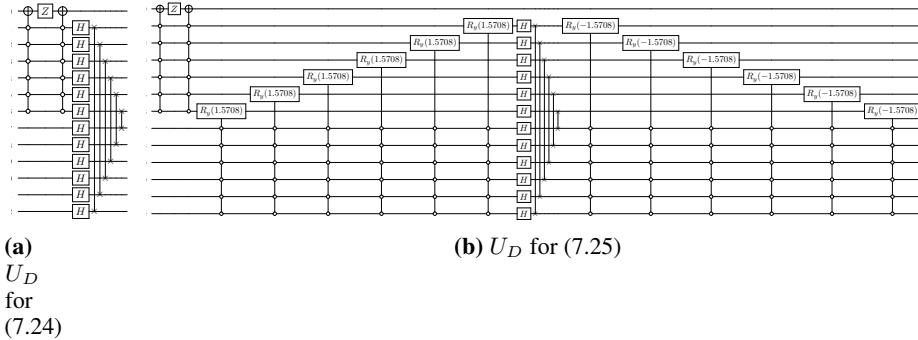


Figure 19. Quantum circuits for block encoding of (7.24) and (7.25).

Starting from the state (7.26), we repeat both circuits for k steps and measure the success probability (7.27). The results of this simulation are shown in Figure 20. We observe that it is sufficient to use a very small k to distinguish the two states, and the two states are maximally distinguishable for k_{opt} given by (7.32) as indicated by the dotted line.

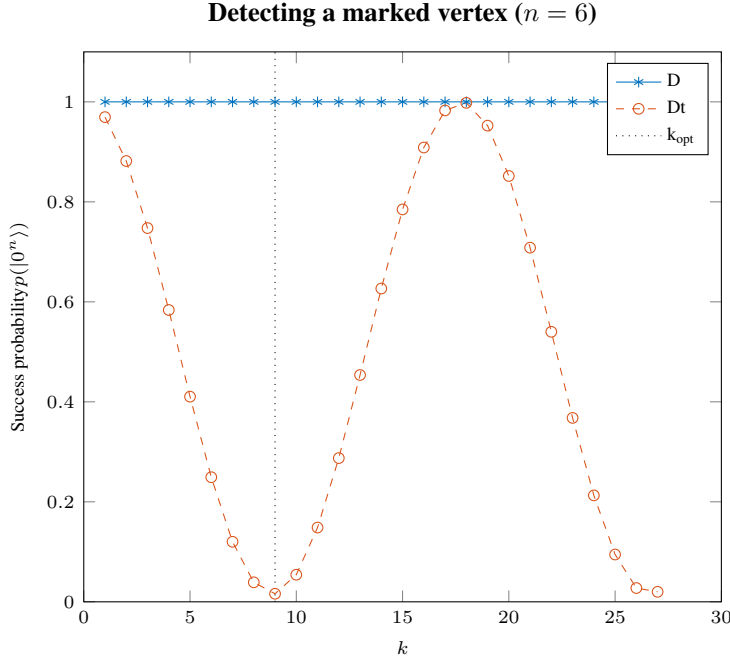


Figure 20. Simulation results for detecting the marked vertex.

References

Guang Hao Low and Isaac L. Chuang. Optimal hamiltonian simulation by quantum signal processing. *Phys. Rev. Lett.*, 118:010501, 2017.

Guang Hao Low and Isaac L Chuang. Hamiltonian simulation by qubitization. *Quantum*, 3:163, 2019.

András Gilyén, Yuan Su, Guang Hao Low, and Nathan Wiebe. Quantum singular value transformation and beyond: exponential improvements for quantum matrix arithmetics. In *Proceedings of the 51st Annual ACM SIGACT Symposium on Theory of Computing*, pages 193–204, 2019.

Lin Lin and Yu Tong. Optimal quantum eigenstate filtering with application to solving quantum linear systems. *Quantum*, 4:361, 2020a.

Lin Lin and Yu Tong. Near-optimal ground state preparation. *Quantum*, 4:372, 2020b.

John M Martyn, Zane M Rossi, Andrew K Tan, and Isaac L Chuang. Grand unification of quantum algorithms. *PRX Quantum*, 2(4):040203, 2021.

Dominic W. Berry, Andrew M. Childs, and Robin Kothari. Hamiltonian Simulation with Nearly Optimal Dependence on all Parameters. *Proceedings - Annual IEEE Symposium on Foundations of Computer Science, FOCS*, 2015-Decem: 792–809, 2015. doi:10.1109/FOCS.2015.54.

Andrew M. Childs, Robin Kothari, and Rolando D. Somma. Quantum algorithm for systems of linear equations with exponentially improved dependence on precision. *SIAM J. Comput.*, 46(6):1920–1950, 2017. doi:10.1137/16M1087072.

D. Camps and R. Van Beeumen. QCLAB, 2021. URL <https://github.com/QuantumComputingLab/qclab>. Version 0.1.3.

Mario Szegedy. Quantum Speed-Up of Markov Chain Based Algorithms. In *45th Annual IEEE Symposium on Foundations of Computer Science*, pages 32–41, 2004. doi:10.1109/FOCS.2004.53.

Andrew M. Childs. On the relationship between continuous- and discrete-time quantum walk. *Comm. Math. Phys.*, 294(2):581–603, 2010. doi:10.1007/s00220-009-0930-1.

J. Haah. Product decomposition of periodic functions in quantum signal processing. *Quantum*, 3:190, 2019.

Rui Chao, Dawei Ding, András Gilyén, Cupjin Huang, and Mario Szegedy. Finding Angles for Quantum Signal Processing with Machine Precision. 2020.

Yulong Dong, Xiang Meng, K Birgitta Whaley, and Lin Lin. Efficient phase factor evaluation in quantum signal processing. *Phys. Rev. A*, 103:042419, 2021.

Lexing Ying. Stable factorization for phase factors of quantum signal processing. *arXiv preprint arXiv:2202.02671*, 2022.

Yulong Dong, Lin Lin, Hongkang Ni, and Jiasu Wang. Infinite quantum signal processing. *arXiv:2209.10162*, 2022.

Jiasu Wang, Yulong Dong, and Lin Lin. On the energy landscape of symmetric quantum signal processing. *Quantum*, 6: 850, 2022.

Daan Camps and Roel Van Beeumen. Fable: Fast approximate quantum circuits for block-encodings. *arXiv preprint arXiv:2205.00081*, 2022.

Mikko Möttönen, Juha J. Vartiainen, Ville Bergholm, and Martti M. Salomaa. Quantum circuits for general multiqubit gates. *Phys. Rev. Lett.*, 93:130502, Sep 2004. doi:10.1103/PhysRevLett.93.130502. URL <https://link.aps.org/doi/10.1103/PhysRevLett.93.130502>.

Eleanor G Rieffel and Wolfgang H Polak. *Quantum computing: A gentle introduction*. MIT Press, 2011.

T D Mackay, S D Bartlett, L T Stephenson, and B C Sanders. Quantum walks in higher dimensions. *Journal of Physics A: Mathematical and General*, 35(12):2745–2753, 2002. doi:10.1088/0305-4470/35/12/304.

S.E. Venegas-Andraca. Quantum walks: a comprehensive review. *Quantum Inf Process*, 11:1015–1106, 2012.

Neil Shenvi, Julia Kempe, and K. Birgitta Whaley. Quantum random-walk search algorithm. *Phys. Rev. A*, 67:052307, 2003. doi:10.1103/PhysRevA.67.052307.

G. Paparo and Martin-Delgado M. Google in a quantum network. *Sci Rep*, 2:444, 2012.

Juha J Vartiainen, Mikko Mötiönen, and Martti M Salomaa. Efficient decomposition of quantum gates. *Phys. Rev. Lett.*, 92(17):1–4, 2004. doi:10.1103/PhysRevLett.92.177902.

Jessica Lemieux, Bettina Heim, David Poulin, Krysta Svore, and Matthias Troyer. Efficient Quantum Walk Circuits for Metropolis-Hastings Algorithm. *Quantum*, 4:287, June 2020. ISSN 2521-327X. doi:10.22331/q-2020-06-29-287. URL <https://doi.org/10.22331/q-2020-06-29-287>.

T Loke and J B Wang. Efficient quantum circuits for Szegedy quantum walks. *Ann. Physics*, 382:64–84, 2017. doi:10.1016/j.aop.2017.04.006.

Ewin Tang. Quantum principal component analysis only achieves an exponential speedup because of its state preparation assumptions. *Phys. Rev. Lett.*, 127(6):060503, 2021.

Sevag Gharibian and François Le Gall. Dequantizing the quantum singular value transformation: Hardness and applications to quantum chemistry and the quantum pcp conjecture. *arXiv preprint arXiv:2111.09079*, 2021.